

# Advancements in Betulinic Acid-Loaded Nanoformulations for Enhanced Anti-Tumor Therapy

Ke Wang<sup>1,2,\*</sup>, Jinlu Shang<sup>3,\*</sup>, Chao Tao<sup>1,2,\*</sup>, Mingquan Huang<sup>4</sup>, Daiqing Wei<sup>5</sup>, Liuxuan Yang<sup>1</sup>, Jing Yang<sup>1</sup>, Qingze Fan<sup>1</sup>, Qian Ding<sup>6</sup>, Meiling Zhou<sup>1</sup>

<sup>1</sup>Department of Pharmacy, the Affiliated Hospital, Southwest Medical University, Luzhou, People's Republic of China; <sup>2</sup>Department of Clinical Pharmacy, School of Pharmacy, Southwest Medical University, Luzhou, People's Republic of China; <sup>3</sup>Department of Pharmacy, West China Hospital Sichuan University Jintang Hospital, Chengdu, People's Republic of China; <sup>4</sup>Sichuan Treatment Center for Gynaecologic and Breast Diseases (Breast Surgery), the Affiliated Hospital, Southwest Medical University, Luzhou, People's Republic of China; <sup>5</sup>Department of Orthopaedics, the Affiliated Hospital, Southwest Medical University, Luzhou, People's Republic of China; <sup>6</sup>Department of Clinical Pharmacy, the Third Hospital of Mianyang, Sichuan Mental Health Center, Mianyang, People's Republic of China

\*These authors contributed equally to this work

Correspondence: Meiling Zhou, Department of Pharmacy, the Affiliated Hospital, Southwest Medical University, No. 25, Taiping Street, Luzhou, Sichuan, 646000, People's Republic of China, Email meilzhou@163.com; Qian Ding, Department of Clinical Pharmacy, the Third Hospital of Mianyang, Sichuan Mental Health Center, No. 190, East Section of Jiannan Road, Mianyang, Sichuan, 621000, People's Republic of China, Email dingqian0506@163.com

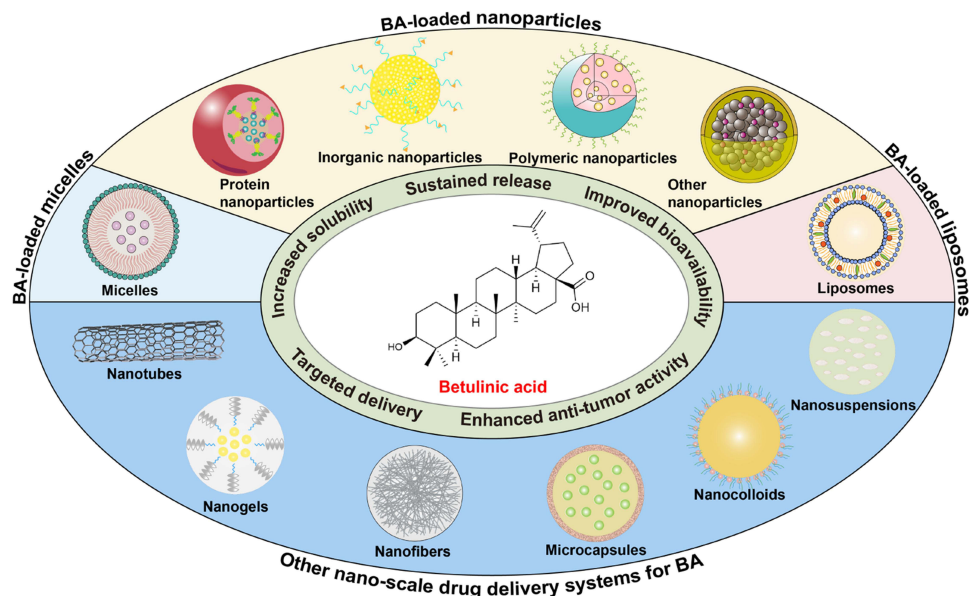
**Abstract:** Betulinic acid (BA) is a natural compound obtained from plant extracts and is known for its diverse pharmacological effects, including anti-tumor, antibacterial, anti-inflammatory, antiviral, and anti-atherosclerotic properties. Its potential in anti-tumor therapy has garnered considerable attention, particularly for the treatment of breast, lung, and liver cancers. However, the clinical utility of BA is greatly hindered by its poor water solubility, low bioavailability, and off-target toxicity. To address these issues, researchers have developed various BA-loaded nanoformulations, such as nanoparticles, liposomes, micelles, and nanofibers, aiming to improve its solubility and bioavailability, prolong plasma half-life, and enhance targeting ability, thereby augmenting its anti-cancer efficacy. In preparing this review, we conducted extensive searches in well-known databases, including PubMed, Web of Science, and ScienceDirect, using keywords like “betulinic acid”, “nanoparticles”, “drug delivery”, “tumor”, and “cancer”, covering the literature from 2014 to 2024. The review provides a comprehensive overview of recent advancements in the application of BA-loaded nano-delivery systems for anti-tumor therapy and offers insights into their future development prospects.

**Keywords:** betulinic acid, nanoformulations, anti-tumor, bioavailability, targeting

## Introduction

BA is a naturally occurring pentacyclic triterpenoid of the lupane type, commonly found in the leaves of *Syzygium jambos*, the bark of *Betula platyphylla*, and the seeds of *Ziziphus jujuba*.<sup>1</sup> BA can be obtained through three primary methods. The most direct approach is extraction from natural plant sources, though this approach exhibits a relatively low yield.<sup>2</sup> The second method is chemical synthesis, where betulin—a structurally similar compound—is often used as a starting material. However, chemical synthesis involves challenges, including harsh reaction conditions and high toxicity.<sup>3</sup> Recently, biotransformation has gained increasing attention for BA production due to its environmental compatibility and milder reaction conditions. Through the development of efficient production strains, biotransformation enables the large-scale production of BA.<sup>4</sup> Numerous studies have reported the diverse pharmacological effects of BA, encompassing anti-tumor,<sup>5</sup> anti-inflammatory,<sup>6</sup> bacteriostatic,<sup>7</sup> anti-atherosclerosis,<sup>8</sup> and anti-osteoporosis activities.<sup>9</sup> In 1976, Trumbull et al first reported the activity of BA against lymphocytic leukemia.<sup>10</sup> Since then, its therapeutic potential for various cancers—such as lung,<sup>11</sup> breast,<sup>12</sup> and liver cancers<sup>13</sup>—has been widely validated in both in vitro and in vivo

## Graphical Abstract



studies. Due to its potent anti-tumor activity and favorable safety profile, the US National Cancer Institute has included BA in its rapid development program.<sup>14</sup>

Particularly in the field of anti-tumor activity, BA demonstrates inhibitory effects on various types of tumors through mechanisms such as affecting the cell cycle, activating apoptotic pathways, and regulating signaling pathways. Its specific mechanisms include inhibiting the formation of the topoisomerase I-DNA cleavable complexes, thereby preventing their involvement in the apoptotic process;<sup>15</sup> inducing tumor cell arrest in the G2/M phase, suppressing DNA synthesis, and activating the mitochondrial apoptotic pathway;<sup>16</sup> promoting tumor necrosis factor-associated apoptosis-inducing ligand production through the p53/caspase-3 signaling pathway;<sup>17</sup> inhibiting vasodilator-stimulated phosphoprotein expression by negatively regulating the NF- $\kappa$ B transcription factors, thereby limiting tumor cell proliferation and migration;<sup>18</sup> activating ferritinophagy-proteins in tumor cells to increase intracellular free iron content, augmenting reactive oxygen species (ROS) production through the Fenton reaction, causing lipid peroxidation in tumor cells, thereby inhibiting their proliferation.<sup>19</sup> Multiple lines of evidence suggest that BA holds great promise as an anti-cancer agent, but its limited water solubility, low bioavailability, and potential off-target toxicity<sup>20</sup> constrain its further application.

In recent years, nano drug delivery systems (NDDSs) have garnered great interest as a strategy capable of substantially increasing drug bioavailability, improving drug targeting, and reducing side effects.<sup>21–23</sup> NDDSs involve the combination of drug molecules with a variety of nanocarriers such as nanoparticles, nanofibers, nanotubes, liposomes, and micelles, which not only improve drug stability and bioavailability but also achieve sustained release and targeted delivery of drugs.<sup>24,25</sup> Currently, extensive research efforts have been devoted to leveraging the advantages of NDDSs to address the shortcomings of BA, aiming to enhance its cellular uptake efficiency, drug accumulation in tumor cells,<sup>26</sup> and capability to cross physiological barriers.<sup>27</sup> In addition, NDDSs can exploit the distinctive properties of nanocarriers, such as pH sensitivity or temperature sensitivity, to achieve drug release under specific conditions, thereby enhancing anti-tumor effects while mitigating toxicity to normal cells.<sup>12</sup>

This review aims to retrospectively review and summarize the recent applications of BA-loaded NDDSs in anti-tumor therapy, with a special focus on how to improve the therapeutic efficacy of BA through nanoformulations. We will also discuss the major challenges existing in current research, including the biocompatibility, stability, and cost-effectiveness of nanocarriers, and look forward to possible future research directions, such as the development of novel nanocarriers

and the integration of nanotechnology with targeted therapeutic strategies. Through this review, our goal is to provide a comprehensive and in-depth reference for the research on the nano delivery of BA and other natural drugs, especially in enhancing their potential application in anti-tumor therapy. We believe that with the continuous progress and deeper exploration of nanotechnology, BA-loaded NDDSs will play an increasingly pivotal role in future anti-cancer treatments.

## BA-Loaded Nanoparticles

Nanoparticles serve as common carriers in NDDSs, significantly enhancing the aqueous solubility, bioavailability, and plasma half-life of drugs, thereby optimizing their pharmacokinetic properties. Nanoparticles can also be modified by targeting ligands on their surface, thereby improving their specific recognition and action on tumor cells. Currently, a variety of BA-loaded nanoparticles have been developed, including protein nanoparticles, inorganic nanoparticles, polymeric nanoparticles, and other nanoparticles, each with unique advantages (Table 1). For instance, Saneja et al<sup>24</sup> successfully prepared PLGA-mPEG nanoparticles loaded with BA using the emulsion solvent evaporation method, which considerably extended the plasma half-life of the drug. In another study, Halder et al<sup>28</sup> coupled BA with lactoferrin (Lf) to obtain Lf-BANp. This formulation not only prolonged the release of BA but also facilitated rapid delivery to MDA-MB-231 and Hep-2 cells, resulting in potent anti-proliferative and cytotoxic effects.

## Protein Nanoparticles

Glycosylated zein (G-zein) exhibits excellent solubility, dispersibility, and bioactivity, which can enhance the stability and encapsulation efficiency of active ingredients.<sup>49</sup> Peng et al<sup>29</sup> successfully prepared G-zein composite nanoparticles loaded with BA (G-zein@BA) using an antisolvent method. G-zein contains abundant hydrophilic groups, and the spatial site-blocking effect introduced by glucose prevents protein aggregation, allowing BA to be tightly encapsulated within G-zein and enhancing its solubility. The interaction between G-zein and BA was facilitated by electrostatic and hydrophobic forces, resulting in an encapsulation efficiency exceeding 80% at a BA concentration of 1 mg/mL. G-zein@BA not only exhibited superior slow-release properties than free BA but also effectively suppressed the proliferation of HepG2 cells.

Human serum albumin (HSA) serves as a versatile protein drug carrier, valued for its biocompatibility, biodegradability, and non-immunogenicity.<sup>50</sup> The secreted protein acidic and rich in cysteine is often overexpressed in the tumor microenvironment (TME), which exhibits a high affinity for HSA. Therefore, anti-tumor drugs using HSA as a carrier tend to be preferentially taken up by tumor cells.<sup>51</sup> Srivari et al<sup>5</sup> prepared monomeric albumin-bound BA nanoparticles (ABBns) through a self-assembly method, achieving efficient loading of approximately 85% to 90% of BA onto HSA. Sodium cholate, used as a surfactant, shares structural similarities with BA and possesses a high aggregation number, which enhances the solubility of BA. Moreover, ABBns exhibited selective uptake by A549 cells and demonstrated high cytotoxicity. Bovine serum albumin (BSA) and HSA share up to 76% similarity in their amino acid sequence,<sup>52</sup> enabling them to effectively bind various albumin receptors overexpressed on the tumor cell surface, such as gp60 and secreted protein acidic and rich in cysteine, thereby enhancing the cellular uptake and therapeutic efficacy of nanoparticles.<sup>53</sup> In their work, Dai et al<sup>30</sup> employed self-assembled BSA-poly(L-lactic acid) as a carrier and successfully prepared BA-loaded nanoparticles via a nanoprecipitation method, which significantly prolonged the blood circulation half-life and anti-tumor activity of BA.

## Inorganic Nanoparticles

Inorganic nanoparticles, which may contain metal ions such as iron, manganese, and gold, have become a focus of research due to their ability to enhance anti-tumor effects through catalyzing specific Fenton reactions in the TME. For instance, Hussein-Al-Ali et al<sup>31</sup> successfully synthesized BA-CS-MNP nanocomposites by coating chitosan (CS) on Fe<sub>3</sub>O<sub>4</sub> magnetic nanoparticles (MNPs) and loading with BA. The resulting composites exhibited a significantly reduced average size of 23.6 nm compared to the 39.6 nm of bare MNPs, attributed to the prolonged high-speed stirring of the polymer and drug after mixing. BA-CS-MNP not only extended the release of BA but also exhibited higher tumor inhibition efficiency. In another investigation, Urandur et al<sup>12</sup> employed a lyotropic liquid crystalline nanostructures (LCN) strategy to incorporate BA and manganese oxide nanoparticles into a dispersion containing phytantriol, Mn-

**Table 1** Summary of BA-Loaded Nanoparticles

Classification	Materials/co-delivery/targeting moiety	Preparation approach	Physico-chemical characteristics	Cells	Animal model	Major outcomes	Ref.
Protein nanoparticles	HSA, Tween 20, sodium cholate	Self-assembled	PS: 10–20 nm ZP: / EE: / DL: 85–90%	A549; Caco-2	/	Increased solubility	[5]
	Glycosylated zein	Antisolvent method	PS: 139.3 ± 0.2 nm ZP: −22.65 ± 1.65 mV EE: 89.81 ± 0.79% DL: /	HepG2	/	Improved dispersion and solubility; sustained drug release	[29]
	BSA, L-LA	Nanoprecipitation method	PS: 118.32 ± 36.26 nm ZP: / EE: / DL: 13.55 ± 1.35%	LLC; A549	LLC subcutaneous tumor xenograft model	Extended half-time; enhanced anti-tumor effects; reduced side effects	[30]



Inorganic nanoparticles	Manganese-oleate complex, phytantriol, pluronic F127	/	PS: $195 \pm 4$ nm ZP: $-18 \pm 3$ mV EE: $96 \pm 3\%$ DL: /	4T1; MDA-MB-231; HEK-293	4T1 tumor xenograft mouse model	Enhanced cytotoxicity; selective breast cancer imaging; synergistic anti-tumor activity	[12]
	Fe <sub>3</sub> O <sub>4</sub> nanoparticles, chitosan	Solution stirring method	PS: 23.6 nm ZP: 25.8 mV EE: / DL: /	3T3; MCF-7	/	Enhanced cytotoxicity	[31]
	Gold nanoparticles, cysteamine	Chemical coupling method	PS: $63 \pm 5.7$ nm ZP: $-27.2 \pm 0.7$ mV EE: / DL: $31.6 \pm 0.24\%$	HaCaT; RPMI-7951	/	Enhanced cytotoxicity via pro-apoptotic effects	[32]
	PLL-g-PEG, HAuCl <sub>4</sub> ·3H <sub>2</sub> O, EGCG (targeting moiety: TPP)	Synthesis method	PS: $119.2 \pm 3.5$ nm ZP: $23.4 \pm 0.5$ mV EE: / DL: $21.0 \pm 0.7\%$	Caco-2; HeLa; MCF-7; HEK293	/	Mitochondrial-targeted delivery; improved cytotoxicity	[33]
	Zn:MnO <sub>2</sub> nanocomposite, polylactic acid, alginate, gallic acid (co-delivery: ceranib-2)	Evaporation-assisted encapsulation method	PS: $84.38 \pm 18.5$ nm ZP: $-34 \pm 6.03$ mV EE: / DL: /	PC-3; HUVEC	/	Exhibited selective cytotoxicity against prostate cancer cells	[34]

(Continued)

Table I (Continued).

Classification	Materials/co-delivery/targeting moiety	Preparation approach	Physico-chemical characteristics	Cells	Animal model	Major outcomes	Ref.
Polymeric nanoparticles	PLGA-mPEG, PVA	Emulsion solvent evaporation method	PS: $147.86 \pm 7.68$ nm ZP: $-5.85 \pm 0.51$ mV EE: $79.18 \pm 5.76\%$ DL: $9.89 \pm 0.72\%$	MCF7; PANC-1	Ehrlich tumor-bearing mouse model	Improved cytotoxicity; long-circulating; enhanced anti-tumor efficacy	[24]
	PLGA, pluronic F127 (targeting moiety: lactoferrin)	Emulsion solvent diffusion technique	PS: $147.7 \pm 6.20$ nm ZP: $-28.51 \pm 3.52$ mV EE: $75.38 \pm 2.70\%$ DL: $4.5 \pm 0.12\%$	MDA-MB-231; HEP-2	/	Cancer cell targeting; increased cytotoxicity and cellular uptake	[28]
	Polyprenol lipid, Vitamin E-TPGS (co-delivery: $C_{60}(OH)_n$ )	Ultrasonic-assisted emulsification method	PS: $191.1 \pm 21.2$ nm ZP: $-6.80 \pm 0.78$ mV EE: $92.89 \pm 5.21\%$ DL: $9.059 \pm 0.598\%$	MHCC97H; L02	/	Enhanced solubility; prolonged drug release; synergistic anti-tumor activity; reduced cytotoxicity for normal cells	[35]
	Microcrystalline cellulose, poly(L-Lactic acid)	Nanoprecipitation method	PS: $135.16 \pm 9.16$ nm ZP: / EE: / DL: $25.68 \pm 2.03\%$	A549; LLC	LLC tumor xenograft model	Enhanced anti-tumor activity; reduced side effects	[36]
	PLGA, PVA	Emulsification and solvent evaporation methods	PS: $257.1$ nm ZP: $-0.170$ mV EE: $84.56 \pm 3.96\%$ DL: $11.13 \pm 0.60\%$	HepG2	Nitrosodiethyl amine-induced hepatocellular carcinoma mice	Improved oral bioavailability; enhanced anti-hepatocellular carcinoma efficacy	[37]

PEG, PBUx-COOH (targeting moiety: FA)	Self-assembly	PS: 152.9 nm ZP: / EE: / DL: 32.7 wt%	HeLa; A549	/	Cancer cell targeting; pH-responsive drug release; enhanced cytotoxicity	[38]
Pillar[6]arene (co-delivery: glucose oxidase)	Self-assembly	PS: 124.78 nm ZP: -25.01 mV EE: / DL: /	MCF-7; A549	/	GSH and ROS dual-responsive drug release; enhanced combined anti-tumor effects	[39]
PLGA-mPEG (co-delivery: GEM)	Double emulsion method	PS: 195.93 ± 6.83 nm ZP: -4.05 ± 0.47 mV EE: / DL: 23.7 ± 0.83%	Panc1	Ehrlich tumor-bearing mouse model	Enhanced cytotoxicity; improved synergistic anti-tumor efficacy	[40]
F-8arm-PEG-BA (co-delivery: HCPT; target moiety: FA)	Nanoprecipitation method	PS: 125.73 ± 20.52 nm ZP: 8.61 ± 0.35 mV EE: / DL: 17.91 ± 1.29%	LLC; A549	LLC xenograft tumor-bearing mice	Extended circulation; tumor targeting; pronounced synergistic anti-cancer effects	[41]
EGCD, TiO <sub>2</sub> nanoparticles, gelatin (targeting moiety: RGD peptide)	Self-assembly	PS: 293.7 nm ZP: 35.76 mV EE: 95.37% DL: /	CCD-11lu; MCF-7; 4T1	4T1 tumor-bearing mice	Improved bioavailability; tumor targeting; improved anti-tumor effects	[42]
MCC, 2-Bromopropionyl bromide, MMA	Nanoprecipitation method	PS: ~120 nm ZP: / EE: / DL: ~20%	B16	B16 tumor-bearing model	Improved cytotoxicity; enhanced anti-tumor effects	[43]

(Continued)

Table 1 (Continued).

Classification	Materials/co-delivery/targeting moiety	Preparation approach	Physico-chemical characteristics	Cells	Animal model	Major outcomes	Ref.
Other nanoparticles	PVA	Standard emulsion approach	PS: 60 nm ZP: -6.78 mV EE: / DL: /	U87; A172	U87 intracranial xenograft tumor-bearing mouse model	Improved cytotoxicity; higher anti-glioma effects	[27]
	Ginsenoside Rb1	Nanoprecipitation method	PS: 103.5 ± 12.7 nm ZP: -14.8 ± 0.5 mV EE: / DL: 35.15 ± 2.76%	LLC; A549	LLC subcutaneous tumor xenograft model	Enhanced anti-tumor effects; green preparation	[44]
	CMC-Na, NH <sub>2</sub> -PEG-COOH, (co-delivery: HCPT; target moiety: FA)	Nanoprecipitation method	PS: 186.23 ± 10.52 nm ZP: / EE: / DL: 22.88 ± 2.05%	LLC; A549	LLC subcutaneous tumor xenograft model	Improved cytotoxicity; enhanced anti-tumor effects; high synergistic effects	[45]
	CuCl <sub>2</sub> 2H <sub>2</sub> O (co-delivery: OA, Ce6)	Reprecipitation method	PS: 174.5 ± 5.3 nm ZP: -31.7 mV EE: / DL: /	4T1	4T1 tumor-bearing mouse model	Tumor targeting, synergistic anti-cancer activity	[46]
	COS (co-delivery: Ce6)	Reprecipitation method	PS: 182 nm ZP: -5.38 mV EE: / DL: /	MCF-7; LO2; HepG2; 4T1; L929	4T1 tumor-bearing mouse model	pH-responsiveness; enhanced synergistic anti-tumor activity	[47]
	Porphyrin derivative	Reprecipitation method	PS: 91.62 nm ZP: -22 mV EE: / DL: /	4T1	/	GSH-responsive drug release; synergistic chemo- and photodynamic therapy	[48]

**Abbreviations:** “/”, means not mentioned in the literature; PS, particle size; ZP, zeta potential; EE, entrapment efficiency; DL, drug loading capacity; HAS, human serum albumin; BSA, bovine serum albumin; L-LA, L-Lactide; PLL-g-PEG, poly-L-lysine-graft-polyethylene glycol; EGCG, epigallocatechin gallate; TPP, triphenylphosphine; PLGA, poly(lactide-co-glycolide); PEG, polyethylene glycol; PVA, polyvinyl alcohol; Vitamin E-TPGS, D- $\alpha$ -tocopherol polyethylene glycol 1000 succinate; PBuOx-COOH, carboxylgroup-terminated poly[2-(3-butenyl)-2-oxazoline]; FA, folate; GSH, glutathione; ROS, reactive oxygen species; GEM, gemcitabine; F-8arm-PEG-BA, folate-conjugated eight-arm-polyethylene glycol-betulinic acid; HCPT, hydroxycamptothecin; EGCD, ethylenediamine- $\gamma$ -cyclodextrin; MCC, microcrystalline cellulose; MMA, methyl methacrylate; CMC-Na, sodium carboxymethylcellulose; OA, oleanolic acid; Ce6, chlorin e6; COS, chitosan oligosaccharide.

Oleate complex, and Pluronic F127. Following storage at room temperature under light protection for three days to reach equilibrium, LCN@Mn-BA was obtained after sonication, enabling selective cancer imaging and therapy. LCN@Mn-BA acted as both a fluorophore and a source of manganese ( $\text{Mn}^{2+}$ ), catalyzing Fenton-like reactions to generate hydroxyl radicals within the TME, thereby inducing apoptosis and effectively inhibiting tumor growth. Compared with a free mixture of  $\text{Mn}^{2+}$  and BA, treatment with LCN@Mn-BA notably decreased tumor cell viability from  $40 \pm 5\%$  to  $17 \pm 4\%$ , underscoring its substantial capability to inhibit tumor cell proliferation.

Targeting mitochondria is also a therapeutic strategy for tumor treatment. Gold nanoparticles (GNP) have been identified as inhibitors of mitochondrial respiration. Ghiulai et al<sup>32</sup> successfully synthesized BA-GNP with selective cytotoxicity by grafting BA onto GNP using cysteamine as a linker. BA-GNP downregulated the expression of the anti-apoptotic factor Bcl-2 and upregulated the pro-apoptotic factor Bax, thereby exerting anti-tumor effects. Furthermore, Oladimeji et al<sup>33</sup> prepared epigallocatechin gallate (EGCG)-coated gold nanoparticles (AuNPs), followed by grafted BA onto AuNPs via a Steglich esterification reaction. Subsequently, the nanoparticles were further coated with poly-L-lysine-graft-polyethylene glycol (PLL-g-PEG) and conjugated with the lipophilic molecule triphenylphosphine ( $\text{TPP}^+$ ), resulting in the formulation T-Au-[PLL-g-PEG]-BA. EGCG exhibits high affinity for the 67 kD laminin receptor on mitochondria, allowing selective uptake of T-Au-[PLL-g-PEG]-BA by 67 kD laminin receptor-overexpressing tumor cells. Cytotoxicity assays conducted on Caco-2, HeLa, and MCF-7 cells revealed that the  $\text{IC}_{50}$  values of T-Au-[PLL-g-PEG]-BA were 3.12, 3.26, and 13.13  $\mu\text{M}$ , respectively, while the  $\text{IC}_{50}$  values of free BA were 9.74, 17.73, and 36.31  $\mu\text{M}$ , indicating the significant anti-tumor effect of T-Au-[PLL-g-PEG]-BA. Further mechanistic studies demonstrated that T-Au-[PLL-g-PEG]-BA achieved substantial inhibition of cancer cell growth through mitochondrial depolarisation, activation of caspases 3/7, and blockade of the G0/G1 phase of the cell cycle.

## Polymeric Nanoparticles

Polymeric nanoparticles composed of hydrophobic and hydrophilic fragments, featuring nanoscale size, high volumetric surface area ratio, and tunable pores, have emerged as pivotal materials in drug delivery.<sup>54</sup> On this basis, Tao et al<sup>35</sup> used Ginkgo biloba Leaves polyphenol and D- $\alpha$ -tocopherol polyethylene glycol 1000 succinate (Vitamin E-TPGS) to construct a core-shell structure and prepared polymeric nanoparticles co-loaded with BA and low-substituted hydroxyl fullerene ( $\text{C}_{60}(\text{OH})_n$ ). TPGS, with its hydrophilic polar head and lipophilic alkyl tail, enhanced the apparent solubility of BA. These nanoparticles effectively suppressed the proliferation of MHCC97H cells by up-regulating the expression of Caspase-3, Caspase-8, and Caspase-9. Moreover, Dai et al<sup>36</sup> prepared cellulose-graft-poly(L-lactic acid) nanoparticles loaded with BA (CE-g-PLLA/BA NPs), which exhibited excellent biocompatibility. The tumor inhibition rate of mice in the CE-g-PLLA/BA NPs group reached 79.8%, markedly surpassing the 46.7% observed in the free BA group, demonstrating enhanced anti-tumor activity. Kumar et al<sup>37</sup> formulated PLGA nanoparticles loaded with BA (BNP) via an emulsion solvent evaporation method. Compared with free BA, BNP prolonged the half-life of BA, elevated blood concentration, and enhanced oral bioavailability, resulting in significant inhibition of HepG2 proliferation. Further studies revealed that BNP induced cell apoptosis by activating the caspase-mediated mitochondrial apoptotic pathway.<sup>13</sup>

Under specific conditions, polymeric nanoparticles can achieve responsive release of BA. Zhang et al<sup>38</sup> developed folate (FA) receptor-targeted polymeric prodrug nanoparticles linked by  $\beta$ -thiopropionate bonds through self-assembly. In the acidic pH of the TME, the  $\beta$ -thiopropionate bonds undergo hydrolysis, enabling responsive release of BA. In another study, Zhu et al<sup>39</sup> utilized ferrocene-modified BA to form host-guest complexes with water-soluble pillar[6]arene and encapsulated glucose oxidase (GOx), resulting in glutathione (GSH)/ROS dual-responsive supramolecular nanoparticles (GOx@BNPs). Activation of GOx@BNPs by overexpressed GSH and ROS in the TME enhanced the release of BA. Furthermore, GOx catalyzed the conversion of glucose to gluconic acid and  $\text{H}_2\text{O}_2$ , where  $\text{H}_2\text{O}_2$  further underwent a Fenton reaction with ferrocene to generate highly active hydroxyl radicals, exerting potent anti-tumor effects. This enables a multimodal synergistic treatment involving chemodynamic therapy (CDT), starvation therapy, and chemotherapy.

Co-delivery of multiple anti-tumor drugs using polymeric nanoparticles can achieve synergistic effects. Saneja et al<sup>40</sup> employed PLGA-mPEG nanoparticles as carriers and co-encapsulated gemcitabine (GEM) and BA to produce combination nanoparticles (GEM + BA NPs). These nanoparticles notably reduced the  $\text{IC}_{50}$  value against Panc1 cells and

displayed significantly higher anti-tumor efficiency compared to the free drugs. In a separate investigation, Dai et al<sup>41</sup> initially synthesized 8arm-PEG-BA by coupling BA with eight-arm-polyethylene glycol carboxylic acid (8arm-PEG-COOH) via an esterification reaction. Subsequent conjugation FA and loading with hydroxycamptothecin (HCPT) yielded F-8arm-PEG-BA/Hcpt nanoparticles, which extended the circulation half-life of BA in the bloodstream. Compared with free BA, F-8arm-PEG-BA/Hcpt nanoparticles exhibited a 76.3-fold increase in cytotoxicity against LLC cells and a 102.6-fold increase against A549 cells, showing significant synergistic effects. Moreover, the PEG shell improved the water solubility of the nanoparticles, while the incorporation of FA conferred tumor-targeting capability. Lu et al<sup>42</sup> employed ethylenediamine- $\gamma$ -cyclodextrin (EGCD) as carriers to encapsulate BA, followed by grafting with gelatin to synthesize BA/GGCD. Using oxidized dextran as a crosslinking agent, BA/GGCD was crosslinked on the surface of the TiO<sub>2</sub> precursor to form a hydrogel (BA/GGNPs) (Figure 1). The introduction of  $\gamma$ -cyclodextrin increased the solubility of BA. BA/GGNPs achieved targeted drug delivery to tumor cells via specific recognition of the RGD sequence, together with the enhanced permeability and retention effect of nanoparticles, resulting in dual-targeting of tumors. In in vivo experiments, BA/GGNPs exhibited excellent tumor inhibition effects, with minimal tumor volume observed in 4T1 tumor-bearing mice after 14 days of treatment, which was further confirmed by histological analysis of tumor slices.

## Other Nanoparticles

The application of green chemistry in NDDSs aims to reduce the utilization of toxic reagents and materials during the preparation process of nanoparticles, thereby minimizing adverse effects on human health and the environment.<sup>44</sup> Self-assembled nanoparticles are stable structures spontaneously formed by organic molecules through non-covalent supramolecular forces, such as hydrophilic-hydrophobic interactions, electrostatic interactions, hydrogen bonds, van der Waals forces, and host-guest interactions. In recent years, nanocarriers derived from natural small molecules with self-assembly capabilities can greatly reduce the use of toxic reagents and exhibit remarkable potential in tumor therapy.

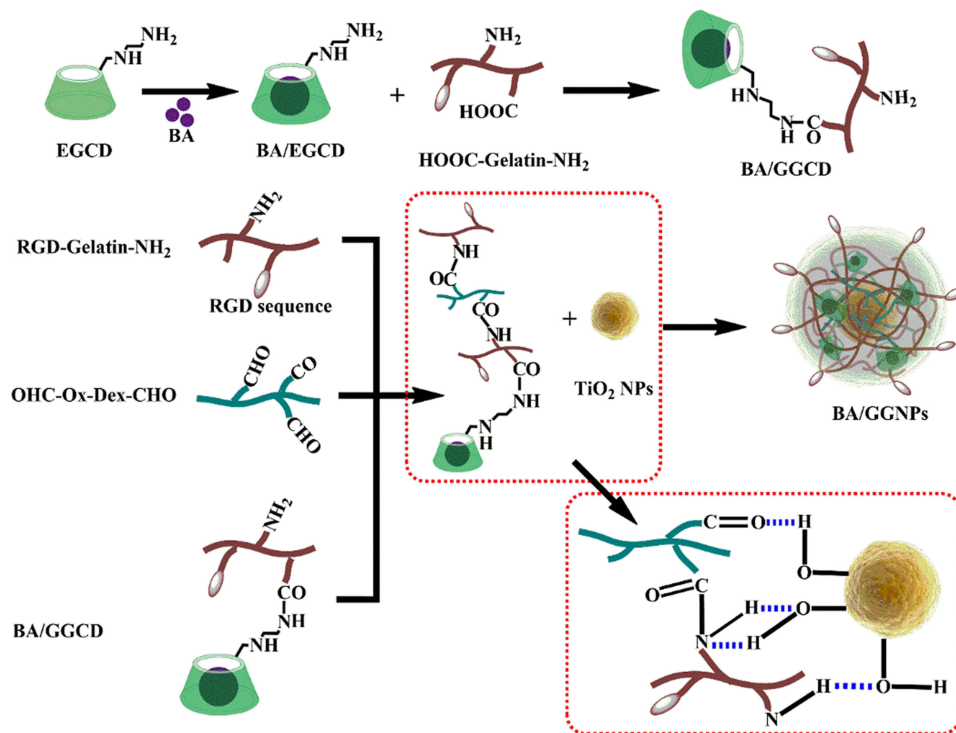


**Figure 1** Schematic illustration depicting the fabrication process of dual-targeted nanoparticles loaded with BA (BA/GGNPs). ACS Appl Bio Mater.

**Notes:** Reprinted from Lu S, Fan X, Wang H et al. Synthesis of gelatin-based dual-targeted nanoparticles of betulinic acid for antitumor therapy. *ACS Appl Bio Mater.* 2020;3(6):3518–3525. Copyright 2020, with permission from the American Chemical Society.<sup>42</sup>

**Abbreviations:** EGCD: ethylenediamine- $\gamma$ -cyclodextrin; GGCD: the compound of gelatin grafted with EGCD; BA/GGNPs: betulinic acid/gelatin- $\gamma$ -cyclodextrin nanoparticles.



Intermolecular hydrogen bonding can drive the self-assembly of BA. Li et al<sup>27</sup> synthesized BA self-assembling nanoparticles (BA NPs), which can inhibit the Akt/NFκB-p65 signaling pathway via CB1/CB2 receptors, arrest the cell cycle at the G0/G1 phase, and effectively induce apoptosis. In a mouse model of intracranial glioblastoma, BA NPs could effectively cross the blood-brain barrier and significantly prolong the mice's survival time. Disulfide bond-driven redox-responsive nanoparticles provide a way to link BA with other drugs. Özdemir et al<sup>48</sup> connected porphyrin derivative (P) with BA via a disulfide bond to obtain redox-responsive nanoparticles (NanoP-ss-BA). In the TME, higher concentrations of GSH triggered disulfide bond cleavage, releasing P and BA, and restoring the photoreactivity of P, thereby promoting ROS production. The zeta potential of NanoP-ss-BA was −22 mV, which contributes to prolonging its circulation half-life and providing excellent stability under physiological conditions. NanoP-ss-BA demonstrated notable chemotoxicity and phototoxicity against cancer cells, which effectively improved the anti-tumor effect of BA. BA can also form conjugates with other components before self-assembly. For example, Dai et al<sup>45</sup> utilized BA as a hydrophobic anti-cancer core to form a conjugate with a hydrophilic shell composed of carboxymethylcellulose (CMC) and PEG-FA and encapsulated HCPT to obtain self-assembled targeted nanoparticles with synergistic anti-tumor effects.

Through co-assembly strategies, better control over the physical size and morphology of the nanocarriers can be achieved to construct multifunctional nano-delivery platforms for synergistic anti-tumor therapy.<sup>55</sup> In this regard, Fu et al<sup>46</sup> initially co-assembled oleanolic acid (OA) and BA, and co-encapsulated Cu<sup>2+</sup> and photosensitizers chlorin e6 (Ce6). Subsequently, the nanoparticles were coated with 4T1 cell membranes to yield CM@OABACe6/Cu nanoparticles. The wrapping of the tumor cell membranes endowed the nanoparticles with excellent homologous tumor targeting, whereas the combination of BA and Ce6 synergistically provided effective chemotherapy and photodynamic therapy (PDT). Considering that the overexpression of GSH in the tumor site partially scavenges ROS, the introduced Cu<sup>2+</sup> can deplete GSH through redox reactions, thus reducing the impact on the PDT effect. In addition, Cu<sup>2+</sup> can undergo a Fenton-like reaction with overexpressed H<sub>2</sub>O<sub>2</sub> in the TME, further augmenting the therapeutic effect. Thus, CM@OABACe6/Cu nanoparticles achieved tumor targeting and triple synergistic treatment involving chemotherapy, PDT, and CDT. As presented in Figure 2A, Cheng et al<sup>47</sup> coupled BA with water-soluble chitosan oligosaccharide (COS) to synthesize amphiphilic COS-BA. Then, a direct co-assembly strategy was employed to introduce the photosensitizer Ce6, constructing water-soluble carrier-free photochemical therapeutic precursors, COS-BA/Ce6 nanoparticles. These nano precursors remained in a “dormant” state in normal tissues but could be activated at the tumor site. Additionally, COS exhibited excellent pH responsiveness and could enhance the immune function of the host by modulating immune cell activity. COS-BA/Ce6 nanoparticles not only enhanced singlet oxygen production but also effectively increased the amount of tumor-derived antigens presented to T cells by combining chemotherapy and PDT. Under the mediation of immune adjuvant anti-PD-L1, COS-BA/Ce6 nanoparticles effectively activated systemic anti-tumor immune response, achieving efficient synergy among chemotherapy, PDT, and immunotherapy. In *in vivo* experiments, 4T1 cells were inoculated on both sides of each mouse. When laser irradiation was performed on only one side of the tumor, both chemotherapy and PDT based on COS-BA/Ce6 nanoparticles effectively activated anti-tumor immunity. After combining with anti-PD-L1 treatment, significant inhibition of the unirradiated side tumors was observed (Figures 2B-2H).

## BA-Loaded Liposomes

Liposomes represent a promising drug delivery system constructed based on lipid bilayers. Encapsulation of hydrophobic drugs within the phospholipid bilayer enhances their solubility, stability, and bioavailability. Table 2 provides an overview of liposomes loaded with BA. Liu et al<sup>56</sup> efficiently synthesized PEGylated BA liposomes through the ethanol injection method. The incorporation of PEG facilitated the formation of an aqueous shell and spatial barriers, resulting in enhanced drug accumulation. *In vitro* release studies demonstrated that PEGylated BA liposomes exhibited sustained drug release. Moreover, cocktail therapy, involving the combination of three or more drugs to reduce resistance, has been explored within liposomal systems. Jin et al<sup>11</sup> prepared cocktail liposomes co-loaded with four natural products, including BA, parthenolide, honokiol, and ginsenoside Rh2, which effectively arrested the G2/M phase of the lung cancer cell cycle. *In vivo* experiments demonstrated superior tumor inhibition rates with the cocktail liposomes compared to individual agents. Intervention in metabolic pathways also has become a noteworthy strategy in tumor therapy. Wang et al<sup>57</sup> utilized a liposomal delivery system to encapsulate BA, yielding BA-NLs for the treatment of colorectal cancer

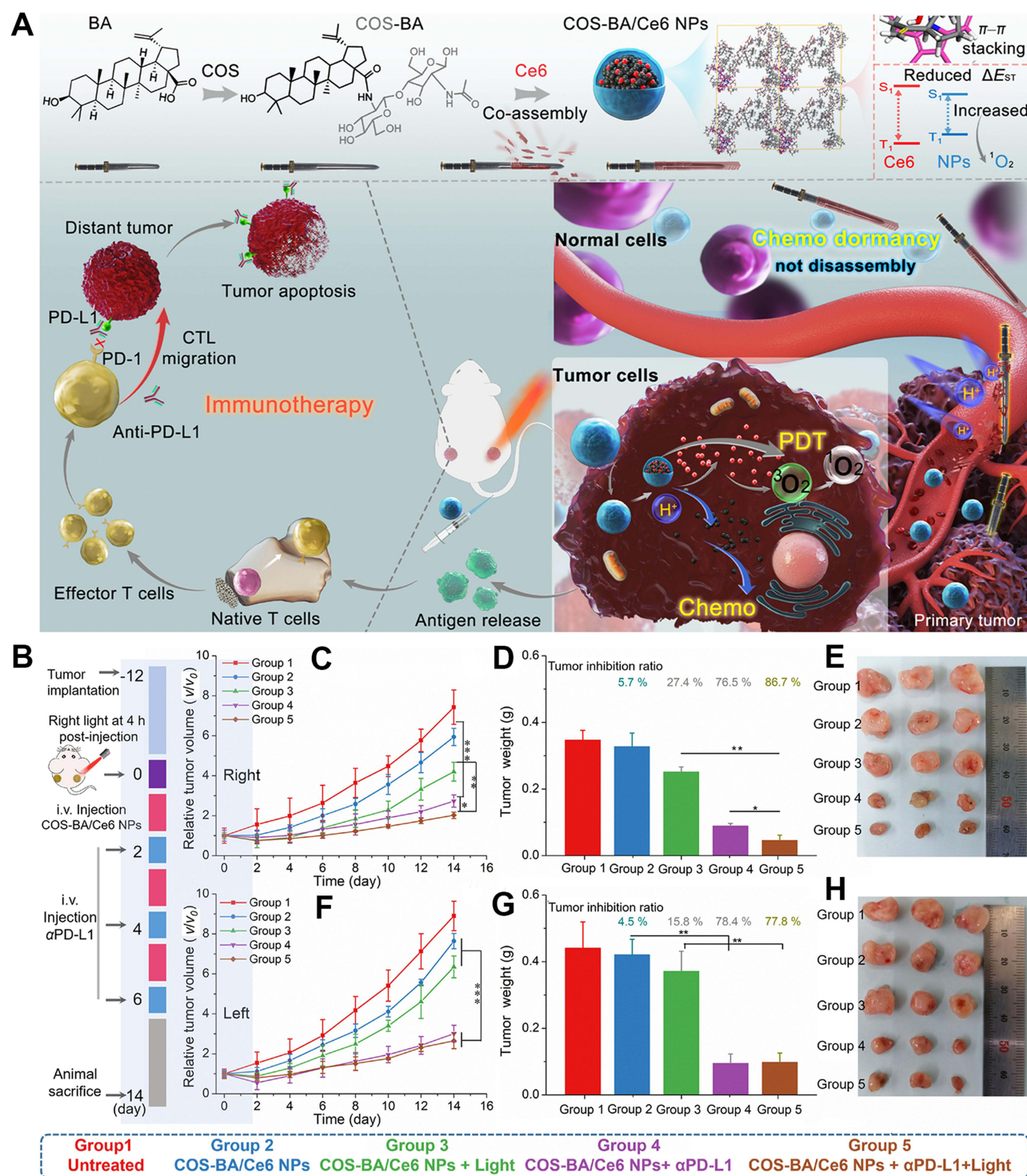


**Figure 2** (A) Schematic diagram of the preparation process and mechanism of COS-BA/Ce6 nanoparticles, showcasing triple synergistic treatment involving chemotherapy, PDT, and immunotherapy. (B) Flowchart of COS-BA/Ce6 nanoparticles-based chemotherapy/PDT with anti-PD-L1 therapy. (C) Tumor growth curves, (D) mean tumor weights, and (E) excised tumor images of the laser-irradiated side of mice after 14 days of treatment. (F) Tumor growth curves, (G) mean tumor weights, and (H) excised tumor images on the unirradiated side of the mice. \* $P < 0.05$ , \*\* $P < 0.01$ , and \*\*\* $P < 0.001$  indicate the statistical significances among groups. Reprinted from Cheng J, Zhao H, Li B et al. Photosensitive pro-drug nanoassemblies harboring a chemotherapeutic dormancy function potentiates cancer immunotherapy. *Acta Pharm Sin B*. 2023;13 (2):879–896.<sup>47</sup>

**Abbreviations:** COS: chitosan oligosaccharide; Ce6: chlorin e6; CTL: cytotoxic T lymphocytes; PDT: photodynamic therapy.

**Table 2** Summary of BA-Loaded Liposomes

Materials/co-delivery/targeting moiety	Preparation approach	Physico-chemical characteristics	Cells	Animal model	Major outcomes	Ref.
Soya lecithin, cholesterol, Tween 80, PEG-2000	Ethanol injection method	PS: 142 nm ZP: / EE: / DL: /	HepG2; HeLa	U14 tumor-bearing mouse model	Prolonged drug release; enhanced bioavailability; increased anti-tumor efficiency	[56]
DSPE-PEG2000, cholesterol, phosphatidylcholine (co-delivery: ginsenoside Rh2, parthenolide, honokiol)	Lipid film hydration method	PS: 115.7 nm ZP: -18.31 mV EE: 89.5% DL: /	A549	A549 xenograft tumor-bearing mouse model	Enhanced synergistic anti-tumor effects; improved anti-tumor efficacy and safety	[11]
Magnetic iron oxides nanoparticles, citric acid, cholesterol, lecithin, DSPE-PEG <sub>2000</sub>	Thin-layer hydration method	PS: 198.1 nm ZP: -19.7 mV EE: 80.54% DL: 7.1%	MCF7; MCF 10A; MDA-MB-231	/	Enhanced cytotoxicity by a combination of hyperthermia with BA	[58]
Soybean lecithin, cholesterol, GSH, Au seed, AuCl <sub>3</sub> , NaBH <sub>4</sub>	Seed-mediated growth method	PS: 149.4 ± 2.4 nm ZP: / EE: 80.6% DL: 8.1%	HeLa; 143B	U14 tumor-bearing mice	Photothermal-responsive drug release; synergistic chemo-photothermal therapy	[59]
GSH, Pd nanoparticles, HAuCl <sub>4</sub>	Seed-mediated growth method	PS: 144.4 nm ZP: / EE: 81.63% DL: /	HeLa	U14 tumor-bearing mice	Photothermal-responsive drug release; synergistic chemo-photothermal therapy	[60]
Egg yolk lecithin, cholesterol, octadecylamine, Tween-80 (targeting moiety: HA)	Ethanol injection method	PS: 155.37 ± 2.25 nm ZP: -18.2 ± 1.57 mV EE: 83.13 ± 2.53% DL: 7.63 ± 0.19%	HepG2; SMMC-7721	/	Cancer cell targeting delivery; enhanced cytotoxicity	[61]

(Continued)

Table 2 (Continued).

Materials/co-delivery/targeting moiety	Preparation approach	Physico-chemical characteristics	Cells	Animal model	Major outcomes	Ref.
FA-PEG <sub>3400</sub> -cholesterol conjugates, egg phosphatidylcholine (target moiety: FA)	Thin lipid film method	PS: 222 ± 8 nm ZP: -20.12 ± 1.45 mV EE: 91.61 ± 1.16% DL: /	HepG2; A549	/	Tumor cell targeting; higher cytotoxicity and cellular uptake	[62]
TPGS, SPC, cholesterol, DSPE-PEG2000-FA (co-delivery: celastrol; targeting moiety: FA)	Thin-film hydration method	PS: 121.3 nm ZP: -15.33 mV EE: 82.77 ± 0.06% DL: 8.46 ± 0.20%	4T1; NIH 3T3	NIH 3T3 + 4T1 orthotopic breast cancer mouse model	Sequential release; inhibited fibrosis; tumor targeting; improved anti-tumor and anti-metastasis effects	[63]
Soybean lecithin, cholesterol, Tween 80 (targeting moiety: cancer cell membrane)	Ethanol injection method and extrusion method	PS: ~150 nm ZP: / EE: 88.03% DL: /	HeLa; L929	/	Tumor cell targeting; enhanced cytotoxicity	[64]
Eudragit S100, soybean lecithin, cholesterol, sodium cholate, isopropyl myristate	Thin film dispersion and pH-driven method	PS: 90.1 ± 21.6 nm ZP: -32 ± 5.1 mV EE: 90.66% DL: /	SW620; HCT116; HT29; SW1116; CT26; HCoEpiC	CT26 tumor-bearing mice	pH-responsive drug release; enhanced cytotoxicity; improved anti-tumor effects	[65]
Soyphosphatidylcholine, cholesterol, mannosylerythritol lipid A	Thin film hydration method	PS: 89.83 ± 0.92 nm ZP: -33.5 ± 2.390 mV EE: 80.44 ± 1.19% DL: /	HepG2	/	Improved cellular uptake; enhanced cytotoxicity	[66]

**Abbreviations:** “/”, means not mentioned in the literature; PS, particle size; ZP, zeta potential; EE, entrapment efficiency; DL, drug loading capacity; PEG, polyethylene glycol; DSPE-PEG2000, 1,2-distearoyl-sn-glycerol-3-phosphoethanolamine-N-[amino (polyethylene glycol)-2000]; GSH, glutathione; HA, hyaluronic acid; FA, folate; TPGS, D- $\alpha$ -tocopherol polyethylene glycol 1000 succinate; SPC, soybean phospholipid.



(CRC). Further studies clarified that BA-NLs inhibit key enzymes in glycolysis, including HK2, PFK-1, PEP, and PKM2, as well as key enzymes in fatty acid metabolism, such as ACSL1, CPT1a, and PEP, thereby exerting a therapeutic effect on CRC.

It has been observed that temperatures of 41–45 °C can markedly reduce the viability of tumor cells,<sup>67</sup> thus rendering hyperthermia a focal point in tumor treatment. Magnetic nanoparticles possess the capability to generate heat under an applied magnetic field, achieving hyperthermia in tumor cells.<sup>68</sup> Within this context, Farcas et al<sup>58</sup> successfully synthesized magnetic iron oxide nanoparticles coated with citric acid (MIONPs\*CA) by the combustion method, using iron nitrate nonahydrate and citric acid monohydrate. Subsequently, they prepared BA-loaded magnetic liposomes (Lip+MIONPs\*CA+BA) using a thin-layer hydration method, which possessed superparamagnetic characteristics and heating abilities. Upon exposure to hyperthermia, these magnetic liposomes underwent a phase transition from gel to liquid, effectively releasing BA and MIONPs for anti-tumor purposes. Additionally, under elevated temperature conditions, the nuclear membrane of MDA-MB-231 cells displayed blistering and morphological alterations, and its microtubule assembly was disrupted, demonstrating the regulatory influence of Lip+MIONPs\*CA+BA on microtubule assembly. Further cytotoxicity assays indicated the enhanced anti-tumor efficacy of the magnetic liposomes against MDA-MB-231 cells induced by hyperthermia, which exhibited greater sensitivity and selective cytotoxicity compared to MCF7 cells.

Photothermal therapy (PTT) is a non-invasive, highly controllable, and precise treatment modality with considerable promise. By modifying targeted ligands on the surface of photothermal materials, active accumulation of drugs in the tumor region can be achieved. Upon near-infrared (NIR) light irradiation, these materials can efficiently convert absorbed light energy into heat, thereby inducing tumor cell death.<sup>69</sup> Gold-based nanomaterials are promising therapeutic agents owing to their exceptional photothermal response properties. Liu et al<sup>59</sup> initially encapsulated BA into liposomes and then seeded Au nanoparticles onto the surface of GSH-modified liposomes via Au-S bonds. Subsequently, they produced gold nanoshell-coated BA liposomes (AuNS-BA-Lips) through the growth of gold nanoshells in a solution containing AuCl<sub>3</sub> and NaBH<sub>4</sub>. These constructs exhibited the ability to be heated up to 43 °C under NIR irradiation and possessed excellent photothermal conversion efficiency. In vitro experiments demonstrated that NIR-excited AuNS-BA-Lips promoted drug uptake by tumor cells, consequently increasing intracellular drug accumulation. Further, in vivo experiments showed that AuNS-BA-Lips exerted remarkably effective anti-tumor effects in mice with tumors, exhibiting an inhibition rate of 83.02%, significantly surpassing the 31.1% inhibition rate observed in the free BA group. These findings suggest that AuNS-BA-Lips possess substantial synergistic therapeutic effects combining chemotherapy and thermotherapy.

Bimetallic nanomaterials based on gold have garnered significant interest owing to their superior stability and enhanced photothermal conversion capabilities compared to monometallic particles. Liu et al<sup>60</sup> used multibranching Au-Pd bimetallic nanoflowers encapsulated with BA liposomes, which provided a high surface area and reactive dendritic tips. The resulting BA-Lips@Pd@Au NFs displayed outstanding photostability and achieved up to 64.6% photothermal conversion efficiency under NIR irradiation, which effectively facilitated their intracellular uptake and demonstrated notable chemo-PTT synergistic therapeutic effects.

The specificity and anti-tumor effect of liposomes on tumor cells can be improved by targeted modifications. Common ligands for targeted modifications include hyaluronic acid (HA), FA, and tumor cell membranes, among others. Wu et al<sup>61</sup> prepared HA-modified BA liposomes (HA-BA-L) using electrostatic interactions. In vitro studies revealed that HA-BA-L inhibited the proliferation of both HepG2 and SMMC-7721 cells more effectively compared to free BA or BA liposomes without HA modification, suggesting its targeted anti-tumor effect. Western blotting results suggested that HA-BA-L inhibited HepG2 cell proliferation by down-regulating intracellular ROCK1, IP3, and RAS expression. FA, a commonly utilized targeting ligand, has demonstrated advantages in improving the efficiency of drug delivery in liposomes. Guo et al<sup>62</sup> successfully prepared FA-functionalized liposomes (FA-L-BA) with targeting ability using FA-PEG3400-cholesterol conjugate. Toxicity assays on HepG2 cells revealed that FA-L-BA displayed stronger cytotoxicity than non-targeted liposomes, demonstrating its targeted anti-tumor effect. In another study, Li et al<sup>63</sup> successfully developed F/CL@BM by co-encapsulating celastrol (CEL) and BA-loaded micelles into liposomes and introducing FA for targeted modification (Figure 3A). FA targeting facilitated drug concentration at the tumor site and sequentially released CEL and BA. CEL can inhibit cancer-associated fibroblasts (CAFs) signal transduction, suppress fibrosis, induce

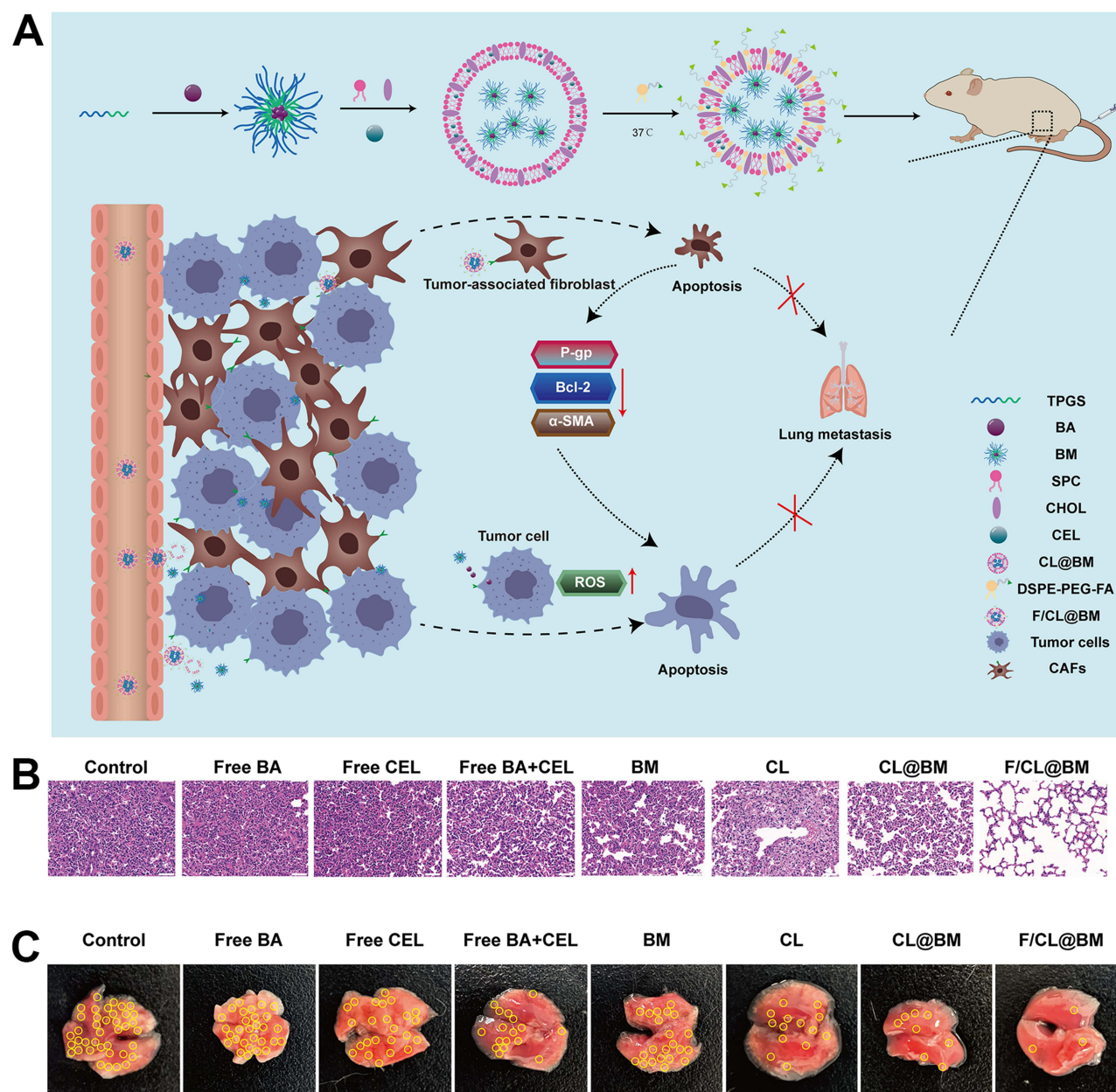


**Figure 3** (A) Schematic diagram of the assembly and mechanism of FA-coated micelles-in-liposomes encapsulating BA and CEL (F/CL@BM) for targeted accumulation at tumor sites and induction of apoptosis in tumor-associated fibroblasts and tumor cells. (B) Representative lung tissue sections stained with hematoxylin and eosin (scale bar: 50 μm). (C) Representative photographs of excised lungs, with tumor nodules circled in yellow. Reprinted from Li C, Wang Z, Zhang Y et al. Efficient sequential co-delivery nanosystem for inhibition of tumor and tumor-associated fibroblast-induced resistance and metastasis. *Int J Nanomed*. 2024;19:1749–1766.<sup>63</sup>  
**Abbreviations:** ROS: reactive oxygen species; TPGS: Vitamin E derivative D-α-tocopherol polyethylene glycol 1000 succinate; BM: BA-loaded micelles; SPC: soybean phospholipid; CHOL: cholesterol; CEL: celastrol; DSPE-PEG-FA: 1,2-distearoyl-sn-glycero-3-phosphoethanolamine-N-[methoxy (polyethylene glycol)-2000]-folic acid; CAFs: cancer-associated fibroblasts; CL: liposomes loaded with CEL.

apoptosis in CAFs, and help reverse tumor resistance to BA. Compared with treatment with the free drug, mice in the F/CL@BM group exhibited a substantial reduction in the number of lung nodules, showing enhanced anti-tumor metastatic effects. Further, in vivo experiments in mice confirmed that F/CL@BM possessed a stronger ability to inhibit tumor growth and could effectively achieve synergistic anti-tumor effects (Figures 3B-3C). Moreover, the strategy of using tumor cell membrane-encapsulated liposomes can effectively combine the advantages of tumor targeting and improved biocompatibility.<sup>70</sup> Chen et al<sup>64</sup> utilized HeLa cell membranes as highly penetrating targeting ligands, and functionalized BA liposomes exhibited significantly enhanced therapeutic efficacy by specifically targeting homologous tumor cells.



Targeted anti-tumor effects can also be achieved by taking advantage of the weak acidity of the TME. Wang et al<sup>65</sup> prepared pH-responsive BA-loaded liposomes (pH-BA-LP) by encapsulating BA into nano-liposomes and introducing Eudragit S100 as an acid-sensitive component. These liposomes exhibited the ability to suppress tumor growth by modulating the Akt/TLR signaling pathway, effectively reducing the migration rate of CRC cells and remarkably down-regulating the expression of NFAT1 and NFAT4 proteins. Additionally, pH-BA-LP demonstrated the capability to enhance the proportion of NK cells and CD3<sup>+</sup> cells in tumor tissues, thus bolstering the autoimmune response and exerting anti-tumor effects.

## BA-Loaded Micelles

Polymer micelles are characterized by their small particle size, which enhances drug solubility, as well as high permeability and retention in tumor tissues, thereby mitigating toxicity.<sup>71,72</sup> Table 3 presents a summary of micelles loaded with BA. Jin et al<sup>73</sup> co-loaded DOX and BA into a pH-sensitive peptide derivatives/DSPE-PEG2000 micelle system. PEGylation prolonged the blood circulation of DOX/BA micelles and improved their accumulation at the tumor site. Upon encountering the acidic TME, the micelles underwent a rapid structural transformation, facilitating efficient drug uptake by tumor cells and stimulating anti-tumor activity. The tumor volume of the DOX/BA micelles group was smaller compared to the free DOX/BA group, suggesting stronger tumor inhibition. Soluplus<sup>®</sup>, an amphiphilic polyvinyl caprolactam-polyvinyl acetate-polyethylene glycol (PVCL-PVA-PEG) graft copolymer, self-assembles to form micelles for drug encapsulation, thereby increasing drug solubility and stability.<sup>74</sup> In another study, Qi et al<sup>75</sup> prepared Soluplus<sup>®</sup>-encapsulated BA micelles (Soluplus<sup>®</sup>-BA), where the carbonyl group of Soluplus<sup>®</sup> formed a hydrogen bond with the hydroxyl group of BA, significantly enhancing its solubility and stability. At a weight ratio of 14:1 for Soluplus<sup>®</sup> and BA, micellar encapsulation reached up to 100%, which effectively avoided drug loss. Soluplus<sup>®</sup>-BA markedly enhanced the anti-tumor effect by increasing the accumulation of intracellular ROS in MDA-MB-231 cells, disrupting mitochondrial membrane potential, and inducing DNA double-stranded breaks. In addition, Soluplus<sup>®</sup>-BA inhibited angiogenesis through modulation of the HIF-1/VEGF-FAK signaling pathway, exerting a multi-mechanism anti-breast cancer effect.

The concentration of GSH in tumor tissues is about 3–4 times higher than the normal tissues, facilitating the cleavage of disulfide bonds through redox reactions,<sup>80</sup> which enabled precise drug release at tumor sites. Zhang et al<sup>76</sup> conjugated BA to PEG polymers via a breakable disulfide bond, successfully preparing a redox-responsive precursor of BA (mPEG<sub>2K</sub>-SS-BA). This conjugation significantly enhanced the saturated solubility of BA, increasing it to 5.7 mg/mL, more than 270 times that of free BA. Subsequently, they formulated P-SS-BA/F68-Cy micelles by self-assembling mPEG<sub>2K</sub>-SS-BA with F68-Cy copolymer coupled with the NIR reagent Cypate. Such micelles exhibited stable colloids with a low critical aggregation concentration. In the high GSH concentration of the TME, P-SS-BA/F68-Cy responsively released BA and exhibited a robust photothermal effect under NIR irradiation, achieving dual-responsive drug delivery and thermo-chemo-therapeutic synergistic treatment. In a study conducted by Qu et al,<sup>77</sup> PEG<sup>5k</sup>-BA<sub>4</sub> was synthesized by conjugating BA to the dendrimeric molecular structure of PEG<sup>5k</sup> via hydrolyzable ester bonds. Subsequently, they cross-linked thiolated dendrimer PEG<sup>5k</sup>-Cys<sub>4</sub>-L<sub>8</sub>-CA<sub>8</sub> with PEG<sup>5k</sup>-BA<sub>4</sub> via disulfide bonds and loaded paclitaxel (PTX) under O<sub>2</sub> mediation, resulting in structurally stable, program-responsive cross-linked micelles (PDCM@PTX) for co-delivery of BA and PTX. The disulfide bonds and hydrolyzable ester bonds within PDCM@PTX micelles enable programmed responses to the overexpressed GSH in the TME and esterases in tumor cells, triggering the release of BA and PTX, thereby demonstrating significant therapeutic effects against multidrug-resistant ovarian cancer. Gautam et al<sup>78</sup> prepared novel redox-sensitive micelles (PX/BA-Cys-T-HA) with HA as a targeting ligand, encapsulating BA and PTX, which specifically bound to the CD44 receptor highly expressed on the surface of MDA-MB-231 cells, thereby enhancing micelle uptake (Figures 4A-4B). In the TME, characterized by high GSH concentration, the disulfide bond underwent cleavage, leading to aggregation or disassembly of the micelles, thereby promoting the release of BA and PTX. In MDA-MB-231 cells, PX/BA-Cys-T-HA substantially enhanced cell cycle arrest, improved depolarization of mitochondrial membrane potential, and stimulated the overproduction of ROS. Moreover, in the 4T1 tumor-bearing mouse model, these targeted micelles demonstrated notable tumor growth inhibition (Figures 4C-4D).

**Table 3** Summary of Micelles Loaded with BA

Materials/co-Delivery/Targeting Moiety	Preparation Approach	Physico-Chemical Properties	Cells	Animal Model	Major Outcomes	Ref.
DSPE-PEG2000 (co-delivery: DOX; targeting moiety: RGD)	Film hydration method	PS: $87.3 \pm 9.2$ nm ZP: $-20.68 \pm 2.28$ mV (pH 7.4), $-2.25 \pm 0.23$ mV (pH 6.5) EE: $88.37 \pm 5.29\%$ DL: $4.05 \pm 0.41\%$	Skvo3	Skvo3 tumor-bearing xenograft mice	Tumor targeting ability; pH-responsive drug release; pronounced synergistic anti-tumor effects	<sup>73</sup>
PVCL-PVA-PEG	Film hydration method	PS: $54.77 \pm 1.26$ nm ZP: $-1.78 \pm 0.78$ mV EE: $\sim 100\%$ DL: /	MDA-MB-231; 4T1	4T1 tumor-bearing mouse model	Enhanced cytotoxicity; enhanced anti-tumor and anti-angiogenic effects	<sup>75</sup>
mPEG <sub>2K</sub> -SS-BA prodrugs, F68-Cypate	Self-assembly	PS: 122.2 nm ZP: 0.2 mV EE: / DL: 7.1%	4T1	4T1 tumor-bearing mouse model	Redox/NIR dual-response drug release; synergistic thermo-chemotherapy anti-tumor efficacy	<sup>76</sup>
PEG <sup>5k</sup> -BA <sub>4</sub> ; PEG <sup>5k</sup> -Cys <sub>4</sub> -L <sub>8</sub> -CA <sub>8</sub> (co-delivery: PTX)	Film hydration method	PS: $81 \pm 3.7$ nm ZP: / EE: / DL: /	A2780/Adr; CP70	A2780/Adr and CP70 tumor-bearing mice	Situ release of drugs; enhanced therapeutic efficacy in multidrug-resistant ovarian cancer	<sup>77</sup>
BA-Cys-TPGS conjugate, HA-Cys-TPGS conjugate (co-delivery: PTX; targeting moiety: HA)	Solvent evaporation method	PS: $134.13 \pm 2.61$ nm ZP: $-25.37 \pm 1.46$ mV EE: $98.09 \pm 4.06\%$ DL: $19.41 \pm 1.54\%$	MDA-MB-231; 4T1; MCF-7	4T1 tumor-bearing mice	Tumor targeting; redox-responsive drug release; enhanced synergistic anti-tumor activity	<sup>78</sup>
HPMA	Self-assembly	PS: 4.2–42.4 nm ZP: / EE: / DL: /	DLD-1; HT-29; HeLa	HT-29 and DLD-1 tumor-bearing xenograft mice	pH-responsive drug release; enhanced cytotoxicity and tumor accumulation	<sup>79</sup>

**Abbreviations:** “/”, means not mentioned in the literature; PS, particle size; ZP, zeta potential; EE, entrapment efficiency; DL, drug loading capacity; DSPE-PEG2000, 1,2-distearoyl-sn-glycerol-3-phosphoethanolamine-N-[amino (polyethylene glycol)-2000]; DOX, doxorubicin; PVCL-PVA-PEG, polyvinyl caprolactam-polyvinyl acetate-polyethylene glycol; NIR, near-infrared; Cys, cystamine; PTX, paclitaxel; TPGS, D- $\alpha$ -tocopherol polyethylene glycol 1000 succinate; HA, hyaluronic acid; HPMA, N-(2-hydroxypropyl)methacrylamide.

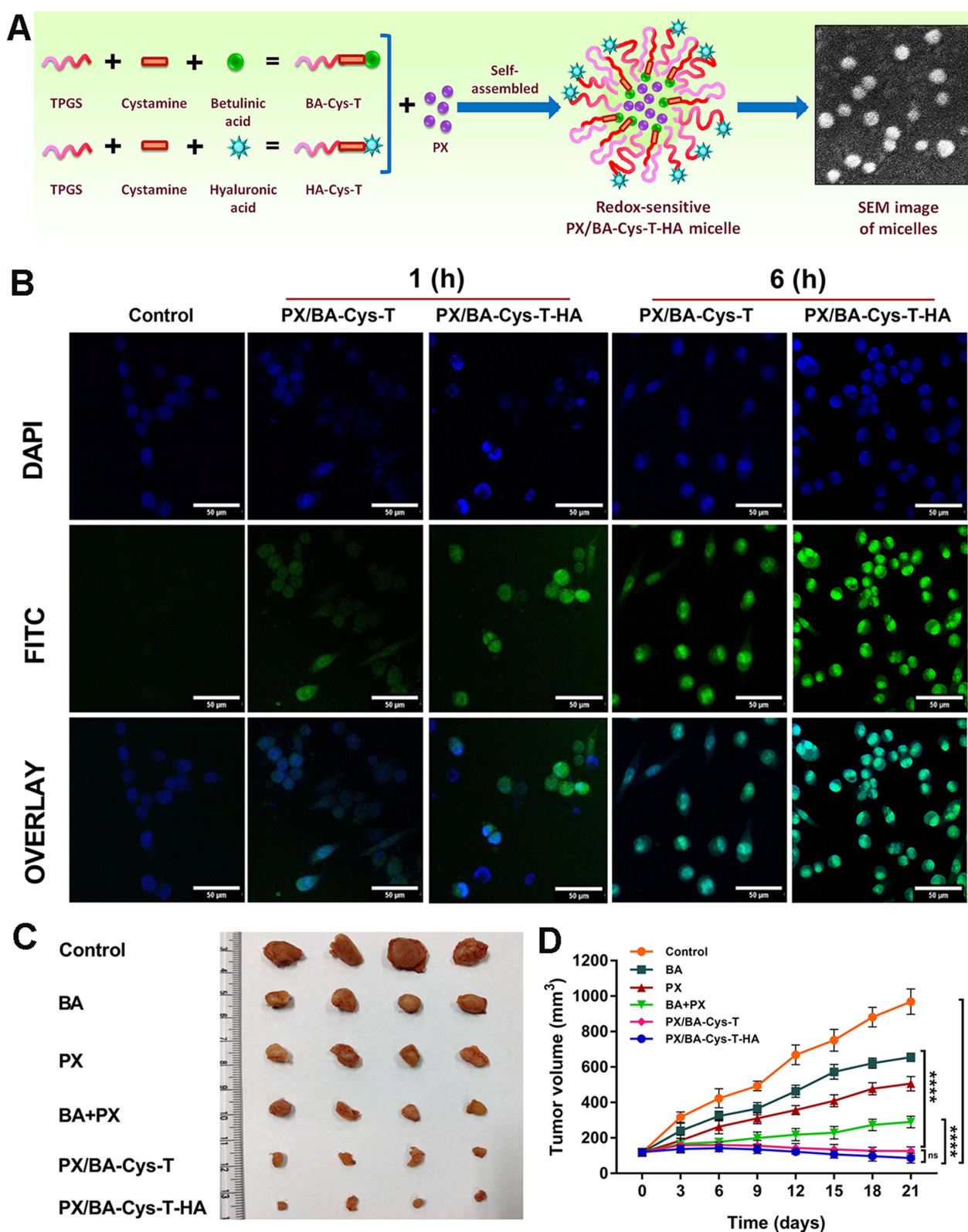


**Figure 4** (A) Flowchart illustrating the preparation of PX/BA-Cys-T-HA micelles. (B) Cellular uptake studies by confocal imaging of FITC-labelled PX/BA-Cys-T-HA acting on MDA-MB-231 cells after 1 and 6 h (scale bar: 50  $\mu$ m). (C) Tumor morphology collected at the end of the in vivo experiment. (D) Tumor volume (mm<sup>3</sup>) plotted against time (days). ns, not significant; \*\*\* $P < 0.0001$  indicate the statistical significances among groups. Reprinted from Gautam S, Marwaha D, Singh N et al. Self-assembled redox-sensitive polymeric nanostructures facilitate the intracellular delivery of paclitaxel for improved breast cancer therapy. *Mol Pharm.* 2023;20(4):1914–1932. Copyright 2023, adapted with permission from the American Chemical Society.<sup>78</sup>

**Abbreviations:** TPMS: D- $\alpha$ -tocopheryl poly(ethylene glycol) succinate; Cys: cystamine; PX: paclitaxel; HA: hyaluronic acid.

## Other Nano-Scale Drug Delivery Systems for BA

Other nano-scale drug delivery systems for BA loading encompass nanotubes, nanogels, nanofibers, microcapsules, nanocolloids, and nanosuspensions (Table 4). These nanoformulations have demonstrated varying degrees of enhancement in the anti-tumor activity of BA.

### Nanotubes

Carbon nanotubes possess a unique three-dimensional tubular structure composed of carbon atoms with  $sp^2$  hybridization. Their remarkable characteristics, including ultra-lightweight, high specific surface area, and excellent biocompatibility, position them as innovative nanocarriers in drug delivery.<sup>91</sup> In a study performed by Tan et al,<sup>81</sup> MWCNT-BA was synthesized by effectively attaching BA to the outer wall of oxidized multiwalled carbon nanotubes (MWCNT-COOH) via  $\pi$ - $\pi$  stacking, resulting in delayed release of BA. In vitro assays demonstrated that the  $IC_{50}$  values of the MWCNT-BA group against A549 and HepG2 cell lines were 2.7 and 11.0  $\mu\text{g/mL}$ , respectively, significantly lower than those of 3.5 and 15.0  $\mu\text{g/mL}$  in the free BA group, indicating enhanced anti-cancer activity. To improve biocompatibility while preserving the activity of BA, the same team<sup>92</sup> further synthesized BA-loaded single-walled carbon nanotubes (SWBA) and coated SWBA with Tween 20 (T20), Tween 80 (T80), PEG, and chitosan (CHI), respectively. Compared with uncoated SWBA, all three surface-modified SWBA, except SWBA-PEG, exhibited slow and sustained drug release characteristics. In toxicity tests on mouse embryonic fibroblasts (3T3), SWBA-T20, SWBA-T80, and SWBA-CHI demonstrated excellent biocompatibility, while SWBA-PEG exhibited relatively higher cytotoxicity. This result is consistent with the drug release patterns of the four biopolymers, confirming the significant influence of drug release and surface coating on the cytotoxicity of nanocarriers.

### Nanogels

Hydrogels are multifunctional materials consisting of three-dimensional polymer networks capable of releasing drugs through structural alterations. However, hydrogels typically display poor loading capacity for hydrophobic drugs.<sup>93</sup> In contrast, polymer nanoparticles possess high drug-loading efficiency and extended plasma half-life.<sup>94</sup> Therefore, combining polymer nanoparticles with hydrogels can substantially improve drug delivery efficiency.

Dai et al<sup>82</sup> initially loaded BA onto CMC to obtain the amphiphilic prodrug CMC-BA, which then self-assembled with HCPT to form nanoparticles. Subsequently, these nanoparticles were further combined with  $\alpha$ -cyclodextrin ( $\alpha$ -CD) to create a cellulose hydrogel drug delivery system (CMC-BA/HCPT nanoparticles/ $\alpha$ -CD) by host-guest encapsulation. This hydrogel exhibited thermo-sensitivity, allowing for reversible gel-sol phase transition at specific temperatures, enabling precise control of drug release. In vitro and in vivo investigations demonstrated that the CMC-BA/HCPT nanoparticles/ $\alpha$ -CD hydrogel exhibited superior therapeutic efficacy over free drugs with enhanced anti-tumor capabilities. Furthermore, the same team explored the substitution of CMC with 8arm-PEG-COOH, which was coupled with BA through esterification to yield 8arm-PEG-BA. Subsequently, this compound self-assembled with HCPT to form micelles, followed by mixing with  $\alpha$ -CD to prepare a novel injectable supramolecular hydrogel (8arm-PEG-BA/HCPT hydrogel). In vitro experiments revealed that 8arm-PEG-BA/HCPT hydrogel exerted the strongest cytotoxicity, attributed to the slow drug release. Additionally, in vivo studies confirmed the enhanced anti-tumor efficacy of this hydrogel compared to free drugs and BA/HCPT-loaded micelles.<sup>83</sup> Thus, injectable hydrogels with unique structures and temperature responsiveness hold promise as potential candidates for the smart delivery of natural drugs.

### Nanofibers

In the field of tumor therapy research, Dash et al<sup>84</sup> developed nanofibers by coupling PEG with depolymerized BA self-assembled fibers (SA-BA), followed by the introduction of FA to augment targeting ability. The resultant FA-PEG-SA-BA exhibited excellent biocompatibility and could be significantly internalized by FA receptor-overexpressing K562 cells, thereby demonstrating selective cytotoxicity. Further investigations revealed<sup>95</sup> that the cytotoxicity of SA-BA was achieved by altering the cellular redox balance, disrupting mitochondrial outer membrane potential, increasing pro-inflammatory cytokine secretion, and enhancing tumor necrosis factor  $\alpha$ -mediated cell death. Additionally,

**Table 4** Other Nano-Scale Drug Delivery Systems for BA

Classification	Materials/co-treatment/ targeting moiety	Preparation approach	Physico-chemical properties	Cells	Animal model	Major outcomes	Ref.
Nanotubes	MWCNT-COOH	Self-assembled	PS: / ZP: / EE: / DL: 14.5–14.8 wt%	3T3; HepG2; A549	/	Enhanced solubility and cytotoxicity	<a href="#">81</a>
Nanogels	CMC-BA prodrug, $\alpha$ -cyclodextrin (co-delivery: HCPT)	Host-guest inclusion complexation	CMC-BA/HCPT nanoparticles: PS: $168.5 \pm 8.1$ nm ZP: / EE: / DL: $22.95 \pm 2.77\%$	LLC	LCC tumor xenograft model	Thermosensitive; extends drug release; enhanced anti-tumor effect	<a href="#">82</a>
	8arm-PEG-BA prodrug, $\alpha$ - cyclodextrin (co-delivery: HCPT)	Host-guest inclusion complexation	PS: / ZP: / EE: / DL: 0.85%	LCC	LCC tumor xenograft model	Thermosensitive; sustained drug release; enhanced anti-tumor effect	<a href="#">83</a>
Nanofibers	PEG <sub>6000</sub> (targeting moiety: FA)	Self-assembled	PS: 92.39 nm ZP: $-25.6$ mV EE: 96.22% DL: 83.66%	KG-1A; K562; RAW 264.7	/	Improved cytotoxicity and cellular uptake	<a href="#">84</a>
	None	Self-assembled	Cross section: 10–25 nm Length: 100 nm–3 $\mu$ m ZP: / EE: / DL: /	KG-1A; K562	DLA tumor- bearing mouse model	Enhanced anti-tumor effect through augmenting immunomodulatory activity	<a href="#">85</a>
Microcapsules	Alginate; guar gum; flaxseed oil; Pluronic F127 (co-delivery: hesperidin)	Spray-drying method	Nanoemulsions: PS: $201 \pm 5$ nm ZP: $-29.4 \pm 0.8$ mV EE: $99.76 \pm 0.22\%$ DL: /	HL-60; L-929	Zebrafish model	Sustained drug release; enhanced biological safety	<a href="#">86</a>

(Continued)

Table 4 (Continued).

Classification	Materials/co-treatment/ targeting moiety	Preparation approach	Physico-chemical properties	Cells	Animal model	Major outcomes	Ref.
Nanocolloids	Trisodium citrate, sodium lauryl sulfate, silver nitrate, PEG	Synthesis method	PS: $71 \pm 3.06$ nm ZP: $-23.6 \pm 0.04$ mV EE: / DL: $61.9 \pm 3.06\%$	HepG2; A549	/	Improved solubility and enhanced anti-tumor activity	<sup>87</sup>
Nanosuspensions	Polyvinyl pyrrolidone, sodium dodecyl sulfate	Anti-solvent precipitation method	PS: $129.7 \pm 12.2$ nm ZP: $-28.1 \pm 4.5$ mV EE: / DL: /	HeLa; A549; HepG2	/	Improved dissolution rate; enhanced cytotoxicity	<sup>88</sup>
	Poloxamer 188, lecithin (co-delivery: PTX)	High-pressure homogenization method	PS: $282.54 \pm 5.4$ nm ZP: $-19.7 \pm 0.19$ mV EE: / DL: /	MCF-7	MCF-7 xenograft tumor-bearing mice	Improved tumor accumulation; synergistic anti-tumor effects	<sup>89</sup>
	Poloxamer 188, lecithin (co-treatment: Taxol®)	High-pressure homogenization method	PS: $161.2 \pm 1.9$ , $406.5 \pm 17.1$ , $722.9 \pm 73.7$ nm ZP: $-22.5 \pm 0.6$ , $-24.6 \pm 0.4$ , $-26.1 \pm 0.1$ mV EE: / DL: /	4T1	4T1 orthotopic tumor mouse model	Nanoparticles (160 nm) enhanced bioavailability and tumor accumulation; synergistic anti-tumor effects	<sup>90</sup>

**Abbreviations:** “/” means not mentioned in the literature; PS, particle size; ZP, zeta potential; EE, entrapment efficiency; DL, drug loading capacity; MWCNT-COOH, oxidized multiwalled carbon nanotubes; CMC-BA, carboxymethylcellulose-betulinic acid; HCPT, hydroxycamptothecin; 8arm-PEG-BA, eight-arm-polyethylene glycol-betulinic acid; PEG, polyethylene glycol; FA, folate; PTX, paclitaxel.



immunocytochemical studies affirmed that SA-BA could activate the expression of caspase-8 and caspase-3, thereby inducing apoptosis in leukemia cell lines.

In addition to its anti-tumor effects, SA-BA also acts as an immune adjuvant, exerting anti-tumor effects by stimulating macrophages. The same team<sup>85</sup> further investigated the immunomodulatory activity of SA-BA. Macrophages pulse-treated with SA-BA exhibited elevated secretion of pro-inflammatory cytokines, enhanced CD4<sup>+</sup> T-lymphocyte proliferation, significant T-cell stimulating ability, and promoted the production of cytotoxic T-lymphocytes (CTLs). Activated CTLs further demonstrated enhanced tumor cell-killing ability. DOX is a commonly used drug in tumor therapy but exhibits high toxicity to peripheral blood lymphocytes (PBLs). This team<sup>96</sup> found that pretreatment with SA-BA significantly decreased pro-inflammatory cytokine levels, improved anti-inflammatory capacity, and protected PBLs from DOX-induced inflammatory responses, thus reducing adverse reactions of DOX. In conclusion, SA-BA not only inhibits tumor cell proliferation but also activates the immune response to suppress tumors while potentially preventing chemotherapy-related serious adverse reactions.

## Microcapsules

Nanocapsules/microcapsules are characterized by high loading capacity, controlled drug release, and targeting ability. Meanwhile, abundant and renewable polysaccharides such as chitosan, alginate, and galactomannan possess excellent biocompatibility and biodegradability. Combining these polysaccharides with nanocapsules/microcapsules yields polysaccharide-based delivery systems, whose dense outer shells can effectively protect the inner core, thereby improving drug delivery efficiency.<sup>97</sup> In this context, Rebouças et al<sup>86</sup> initially formulated nano-emulsions co-loaded with BA and hesperidin by rotary evaporation method, which were further homogeneously mixed with aqueous solutions of alginate and guar gum polysaccharides to obtain polysaccharide microcapsules. Compared with free drugs, these microcapsules exhibited sustained drug release, selective toxicity against tumor cells, and reduced toxicity to non-tumor cells. This improvement in drug safety underscores the potential of polysaccharide-based microcapsules in the field of drug delivery.

## Nanocolloids

Silver nanoparticles (Sil NPs) play an important role in the biomedical field owing to their distinctive physicochemical and biological properties. In particular, Sil NPs exhibit remarkable anti-tumor effects primarily by disrupting the mitochondrial respiratory chain and promoting ROS production.<sup>98</sup> Studies have indicated that combining BA with Sil NPs can further potentiate their anti-tumor ability. In a study conducted by Pinzaru et al,<sup>87</sup> silver nano colloids (SilCo) were successfully synthesized by continuously stirring a mixture comprising trisodium citrate, sodium lauryl sulfate, and silver nitrate solution at 80 °C for 30 min. Subsequently, SilCo was loaded with BA to generate SilCo\_BA. Cytotoxicity assessments performed on HepG2 cells revealed a cell survival rate of 75.30% in the free BA group, while it decreased to 66.44% in the SilCo\_BA group, suggesting an enhanced anti-tumor effect of BA.

## Nanosuspensions

Nanosuspensions refer to nano-sized particles composed solely of pure drugs without any matrix materials and represent an effective strategy to improve the bioavailability of natural drugs.<sup>99</sup> In this regard, Li et al<sup>88</sup> successfully prepared BA nanosuspensions (BA-NS) in a stable amorphous state using an anti-solvent precipitation method. The use of sodium dodecyl sulfate and polyvinyl pyrrolidone K29-32 as stabilizers significantly improved the water solubility of BA. BA-NS exhibited pH-dependent release characteristics, with the release of BA increasing with pH. In addition, BA-NS exhibited enhanced cytotoxicity against HeLa, A549, and HepG2 cells, thereby augmenting the in vitro antiproliferative effect on tumor cells.

Furthermore, Wang et al<sup>89</sup> developed PTX-BA hybrid nanosuspensions (PTX-BA-NP), which co-loaded BA and PTX in the form of nanocrystals. This approach improved the solubility of both drugs and achieved synergistic therapeutic effects against breast cancer. To further investigate the impact of particle size on the anti-breast cancer efficacy of BA-NS, they<sup>90</sup> employed the high-pressure homogenization method to prepare BA-NS with particle sizes of 160, 400, and 700 nm, respectively. Results indicated that BA-NS with a size of 160 nm exhibited a superior drug release rate and bioavailability than the larger particle sizes. It was found that BA-NS could be effectively internalized by 4T1 cells,

resulting in higher levels of intracellular accumulation. Moreover, the combination of 160 nm-sized BA-NS and Taxol<sup>®</sup> demonstrated enhanced anti-tumor ability, effectively exerting a synergistic anti-tumor effect. This series of studies not only confirmed the potential of nanosuspensions in enhancing drug bioavailability but also highlighted the importance of optimizing the anti-tumor activity of nanoparticles by controlling their particle size.

## Summary and Outlook

BA holds promising application prospects due to its outstanding anti-tumor activity, but its clinical utilization is greatly hindered by issues such as poor solubility, low bioavailability, and potential off-target toxicity. To overcome these drawbacks, researchers have encapsulated BA into diverse nanocarriers, including nanoparticles, liposomes, polymer micelles, nanotubes, nanogels, nanofibers, and nanosuspensions. These nanoformulations have demonstrated excellent therapeutic effects against a diverse range of tumors, as depicted in Figure 5A. Notably, breast cancer (22.97%) and lung cancer (21.67%) have received the most attention, followed by liver cancer (16.22%) and cervical cancer (10.81%). Over the past decade, research on BA-loaded nanoformulations for tumor treatment has continued to progress, as illustrated in Figure 5B. These nanoformulations not only substantially enhanced the solubility and bioavailability of BA but also greatly improved its anti-tumor activity through strategies such as controlled release and targeted delivery.

This review focuses on strategies to improve the anti-tumor effect of BA through various nanoformulations. Firstly, by conjugating targeting ligands such as FA and HA onto nanocarriers, tumor cells can be specifically identified, enabling precise treatment and reducing damage to normal cells. Secondly, leveraging the unique properties of the TME, such as its acidic pH and high concentration of GSH, allows for the design of stimuli-responsive nanoformulations. These include pH-responsive and redox-responsive systems, enabling tumor site-specific drug release. In addition, the co-delivery of BA with other anti-tumor drugs, combined with different anti-cancer mechanisms, can synergistically enhance

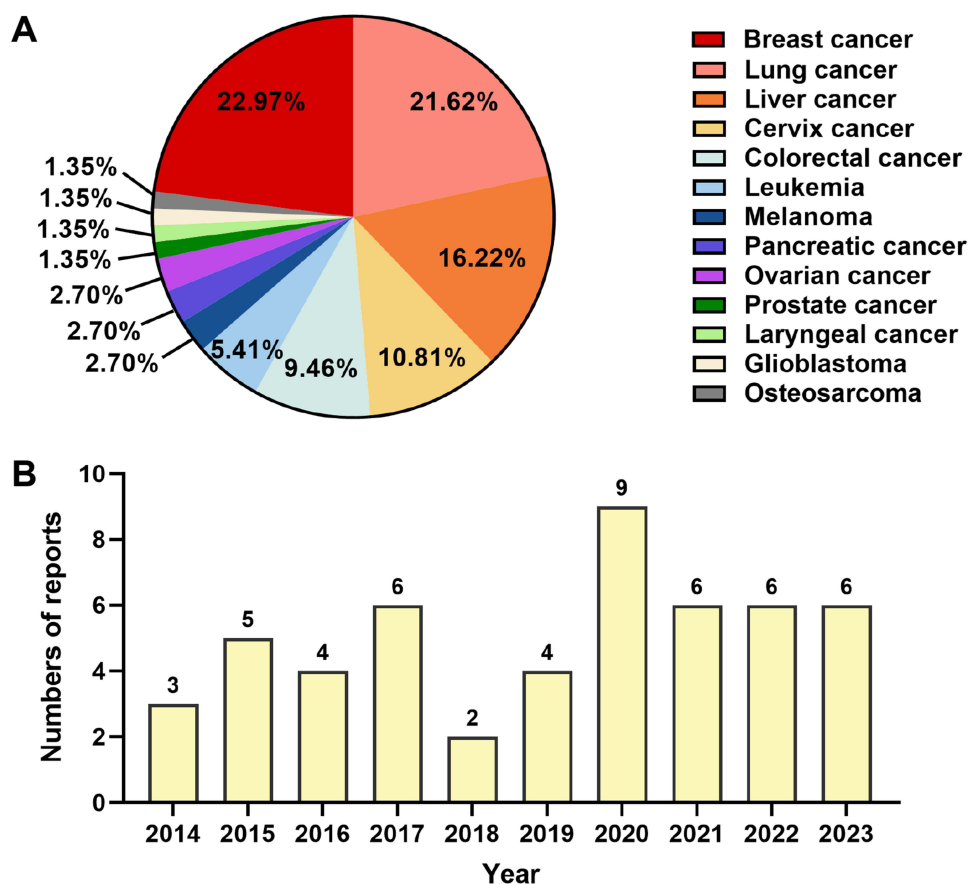


**Figure 5** (A) Application of BA-loaded nanoscale delivery systems across various tumor types. (B) Annual publication trends of BA-loaded nanoformulations.

anti-tumor effects while mitigating or preventing serious adverse reactions associated with chemotherapy. In recent years, PTT and PDT have emerged as effective anti-tumor modalities, and researchers have developed BA-loaded nanopreparations capable of combining PTT and PDT, resulting in significantly enhanced anti-tumor effects.

Despite significant progress has been made in these studies, the translation of BA-loaded nanopreparations from laboratory to clinical applications still faces numerous challenges. Firstly, ensuring the safety of nanocarriers remains a critical issue that needs to be addressed during clinical translation. Comprehensive safety and toxicological studies of BA-loaded nanoformulations are crucial, especially research on long-term toxicity, biodistribution, metabolism, and excretion. Furthermore, some studies have focused on *in vitro* and cell models, lacking sufficient trial data to verify the efficacy and safety of these nanoformulations. Therefore, future investigations should pay more attention to *in vivo* experimental design, such as monitoring the behavior of nanocarriers using advanced imaging techniques. Moreover, a deeper understanding of the anti-tumor mechanisms of BA and its nanoformulations is needed, encompassing elucidating molecular pathways, therapeutic targets, and interactions with the TME. Such insights can facilitate the development of more precise treatment strategies. Finally, the transition from laboratory to industrial-scale production poses a significant challenge. Addressing the stability of formulations during technology transfer and scale-up production is essential for ensuring consistency and efficacy in large-scale production processes.

Future directions also entail the exploration of innovative nanocarrier designs and the development of novel targeting molecules to enhance the efficiency and safety of anti-tumor therapies. Interdisciplinary collaboration, combined with the latest advancements in medicinal chemistry, nanotechnology, and molecular biology, will provide a strong impetus to overcome existing challenges. For instance, medicinal chemistry can contribute to designing more effective targeting ligands and prodrugs, nanotechnology can improve drug loading and release profiles, and molecular biology can help identify precise molecular targets, allowing for highly specific tumor targeting. Additionally, artificial intelligence holds significant potential in advancing nanomedicine, especially in the design and optimization of nanodrugs for tumor therapy. Through predictive modeling, artificial intelligence can rapidly estimate tumor cell uptake and drug release efficiency based on the physicochemical properties of nanomedicines, perform high-speed analysis on complex biological datasets, and generate optimized design schemes, thereby accelerating the research process. Collectively, these interdisciplinary approaches can optimize the design of nano-delivery systems and accelerate their clinical applications.

Since studies on BA-loaded NDDSs are still in their early stages, much of the reported data primarily come from *in vitro* and animal models, with a lack of clinical research data. Therefore, this review is based mainly on existing preclinical research findings, and the clinical translational applicability of these systems needs to be further verified. While this review covers various types of NDDSs, the differing designs, synthesis methods, and efficacy evaluation criteria of these systems make it challenging to directly compare their effects, which may result in the advantages and disadvantages of different systems not yet fully revealed.

In summary, BA-loaded nano-delivery systems demonstrate broad prospects in the field of anti-tumor research owing to their unique therapeutic advantages. Through continuous technological innovation and in-depth research, it is expected that these nano-delivery strategies will be successfully translated into practical clinical applications in the near future, offering more effective and safer therapeutic options for tumor patients.

## Data Sharing Statement

Data will be made available on request.

## Funding

This work was supported by the Luzhou Municipal People's Government-Southwest Medical University Science and Technology Strategic Cooperation Project [grant number 2023LZXNYDJ004] and the National Natural Science Foundation of China [grant number 82104083].

## Disclosure

The authors declare no conflicts of interest in this work.

## References

- Banerjee S, Banerjee S, Bishayee A, et al. Cellular and molecular mechanisms underlying the potential of betulinic acid in cancer prevention and treatment. *Phytomedicine*. 2024;132:155858. doi:10.1016/j.phymed.2024.155858
- Lou H, Li H, Zhang S, Lu H, Chen Q. A review on preparation of betulinic acid and its biological activities. *Molecules*. 2021;26(18):5583. doi:10.3390/molecules26185583
- Jiang W, Li X, Dong S, Zhou W. Betulinic acid in the treatment of tumour diseases: application and research progress. *Biomed Pharmacother*. 2021;142:111990. doi:10.1016/j.biopha.2021.111990
- Jin C, Zhang J, Song H, Cao Y. Boosting the biosynthesis of betulinic acid and related triterpenoids in *Yarrowia lipolytica* via multimodular metabolic engineering. *Microb Cell Fact*. 2019;18(1):77. doi:10.1186/s12934-019-1127-8
- Srivari Y, Chatterjee P. Factors influencing the fabrication of albumin-bound drug nanoparticles (ABDNs): part I. albumin-bound betulinic acid nanoparticles (ABBns). *J Microencapsul*. 2016;33(8):689–701. doi:10.1080/02652048.2016.1222005
- Sosa-Gutierrez DS, Toro-Vazquez JF, Cano-Sarmiento C, et al. Betulinic acid nanogels: rheological, microstructural characterization and evaluation of their anti-inflammatory activity. *Curr Drug Deliv*. 2021;18(2):212–223. doi:10.2174/1567201817999200817154003
- Wang C, Chen H, Wu Z, Jhan Y, Shyu C, Chou C. Antibacterial and synergistic activity of pentacyclic triterpenoids isolated from *Alstonia scholaris*. *Molecules*. 2016;21(2):139. doi:10.3390/molecules21020139
- Zhang J, Almoallim HS, Alharbi SA, Yang B. Anti-atherosclerotic activity of betulinic acid loaded polyvinyl alcohol/methylacrylate grafted lignin polymer in high fat diet induced atherosclerosis model rats. *Arab J Chem*. 2021;14(2):102934. doi:10.1016/j.arabjc.2020.102934
- Sardar A, Gautam S, Sinha S, et al. Nanoparticles of naturally occurring PPAR- $\gamma$  inhibitor betulinic acid ameliorates bone marrow adiposity and pathological bone loss in ovariectomized rats via Wnt/ $\beta$ -catenin pathway. *Life Sci*. 2022;309:121020. doi:10.1016/j.lfs.2022.121020
- Trumbull ER, Bianchi E, Eckert DJ, Wiedhopf RM, Cole JR. Tumor inhibitory agents from *Vauquelinia corymbosa* (Rosaceae). *J Pharm Sci*. 1976;65(9):1407–1408. doi:10.1002/jps.2600650938
- Jin X, Yang Q, Cai N, Zhang Z. A cocktail of betulinic acid, parthenolide, honokiol and ginsenoside Rh2 in liposome systems for lung cancer treatment. *Nanomedicine*. 2020;15(1):41–54. doi:10.2217/nmm-2018-0479
- Urandur S, Banala VT, Shukla RP, et al. Theranostic lyotropic liquid crystalline nanostructures for selective breast cancer imaging and therapy. *Acta Biomater*. 2020;113:522–540. doi:10.1016/j.actbio.2020.06.023
- Kumar P, Gautam AK, Kumar U, et al. Mechanistic exploration of the activities of poly(lactic-co-glycolic acid)-loaded nanoparticles of betulinic acid against hepatocellular carcinoma at cellular and molecular levels. *Arch Physiol Biochem*. 2022;128(3):836–848. doi:10.1080/13813455.2020.1733024
- Ali-Sayed M, Jantan I, Vijayaraghavan K, Bukhari SNA. Betulinic acid: recent advances in chemical modifications, effective delivery, and molecular mechanisms of a promising anticancer therapy. *Chem Biol Drug Des*. 2016;87(4):517–536. doi:10.1111/cbdd.12682
- Ganguly A, Das B, Roy A, et al. Betulinic acid, a catalytic inhibitor of topoisomerase I, inhibits reactive oxygen species-mediated apoptotic topoisomerase I-DNA cleavable complex formation in prostate cancer cells but does not affect the process of cell death. *Cancer Res*. 2007;67(24):11848–11858. doi:10.1158/0008-5472.CAN-07-1615
- Sun Y, Song C, Viernstein H, Unger F, Liang Z. Apoptosis of human breast cancer cells induced by microencapsulated betulinic acid from sour jujube fruits through the mitochondria transduction pathway. *Food Chem*. 2013;138(2–3):1998–2007. doi:10.1016/j.foodchem.2012.10.079
- Xu Y, Li J, Li Q, Feng Y, Pan F. Betulinic acid promotes TRAIL function on liver cancer progression inhibition through p53/caspase-3 signaling activation. *Biomed Pharmacother*. 2017;88:349–358. doi:10.1016/j.biopha.2017.01.034
- Chen X, Yuan X, Zhang Z, et al. Betulinic acid inhibits cell proliferation and migration in gastric cancer by targeting the NF- $\kappa$ B/VASP pathway. *Eur J Pharmacol*. 2020;889:173493. doi:10.1016/j.ejphar.2020.173493
- Xiu Z, Zhu Y, Li S, et al. Betulinic acid inhibits growth of hepatoma cells through activating the NCOA4-mediated ferritinophagy pathway. *J Funct Foods*. 2023;102:105441. doi:10.1016/j.jff.2023.105441
- Dai L, Li D, Cheng J, et al. Water soluble multiarm-polyethylene glycol-betulinic acid prodrugs: design, synthesis, and in vivo effectiveness. *Polym Chem*. 2014;5(19):5775–5783. doi:10.1039/c4py00648h
- Yin W, Li Y, Gu Y, Luo M. Nanoengineered targeting strategy for cancer immunotherapy. *Acta Pharmacol Sin*. 2020;41(7):902–910. doi:10.1038/s41401-020-0417-3
- Li J, Qiang H, Yang W, et al. Oral insulin delivery by epithelium microenvironment-adaptive nanoparticles. *J Control Release*. 2022;341:31–43. doi:10.1016/j.jconrel.2021.11.020
- Zhang Z, Liang X, Yang X, Liu Y, Zhou X, Li C. Advances in nanodelivery systems based on metabolism reprogramming strategies for enhanced tumor therapy. *ACS Appl Mater Interfaces*. 2024;16(6):6689–6708. doi:10.1021/acsami.3c15686
- Saneja A, Kumar R, Singh A, et al. Development and evaluation of long-circulating nanoparticles loaded with betulinic acid for improved anti-tumor efficacy. *Int J Pharm*. 2017;531(1):153–166. doi:10.1016/j.ijpharm.2017.08.076
- Yang J, Zhang R, Wang F, et al. Red blood cell membrane-camouflaged prednisolone acetate-loaded PLGA nanoparticles for kidney-targeted drug delivery. *J Drug Deliv Sci Technol*. 2023;86:104693. doi:10.1016/j.jddst.2023.104693
- Liu Y, Zhang X, Luo L, et al. Gold-nanobranched-shell based drug vehicles with ultrahigh photothermal efficiency for chemo-photothermal therapy. *Nanomedicine*. 2019;18:303–314. doi:10.1016/j.nano.2018.09.015
- Li Y, Wang Y, Gao L, et al. Betulinic acid self-assembled nanoparticles for effective treatment of glioblastoma. *J Nanobiotechnology*. 2022;20(1):39. doi:10.1186/s12951-022-01238-7
- Halder A, Jethwa M, Mukherjee P, et al. Lactoferrin-tethered betulinic acid nanoparticles promote rapid delivery and cell death in triple negative breast and laryngeal cancer cells. *Artif Cells Nanomed Biotechnol*. 2020;48(1):1362–1371. doi:10.1080/21691401.2020.1850465
- Peng F, Jin Y, Wang K, Wang X, Xiao Y, Xu H. Glycosylated zein composite nanoparticles for efficient delivery of betulinic acid: fabrication, characterization, and in vitro release properties. *Foods*. 2022;11(17):2589. doi:10.3390/foods11172589
- Dai L, Li C, Liu K, et al. Self-assembled serum albumin-poly(L-lactic acid) nanoparticles: a novel nanoparticle platform for drug delivery in cancer. *RSC Adv*. 2015;5(20):15612–15620. doi:10.1039/c4ra16346j
- Hussein-Al-Ali SH, Arulselvan P, Fakurazi S, Hussein MZ. The in vitro therapeutic activity of betulinic acid nanocomposite on breast cancer cells (MCF-7) and normal fibroblast cell (3T3). *J Mater Sci*. 2014;49(23):8171–8182. doi:10.1007/s10853-014-8526-3

32. Ghiulai R, Mioc A, Racoviceanu R, et al. The anti-melanoma effect of betulinic acid functionalized gold nanoparticles: a mechanistic in vitro approach. *Pharmaceuticals*. 2022;15(11):1362. doi:10.3390/ph15111362
33. Oladimeji O, Akinyelu J, Daniels A, Singh M. Modified gold nanoparticles for efficient delivery of betulinic acid to cancer cell mitochondria. *Int J Mol Sci*. 2021;22(10):5072. doi:10.3390/ijms22105072
34. Tan E, Danışman-Kalındemirtaş F, Karakuş S. Effective drug combinations of betulinic acid and ceranib-2 loaded Zn:MnO<sub>2</sub> doped-polymeric nanocarriers against PC-3 prostate cancer cells. *Colloids Surf B*. 2023;225:113278. doi:10.1016/j.colsurfb.2023.113278
35. Tao R, Wang C, Lu Y, et al. Characterization and cytotoxicity of polypropylene lipid and vitamin E-TPGS hybrid nanoparticles for betulinic acid and low-substituted hydroxyl fullerene in MHCC97H and L02 Cells. *Int J Nanomed*. 2020;15:2733–2749. doi:10.2147/IJN.S249773
36. Dai L, Yang T, He J, et al. Cellulose-graft-poly(L-lactic acid) nanoparticles for efficient delivery of anti-cancer drugs. *J Mater Chem B*. 2014;2(39):6749–6757. doi:10.1039/c4tb00956h
37. Kumar P, Singh AK, Raj V, et al. Poly(lactic-co-glycolic acid)-loaded nanoparticles of betulinic acid for improved treatment of hepatic cancer: characterization, in vitro and in vivo evaluations. *Int J Nanomed*. 2018;13:975–990. doi:10.2147/IJN.S157391
38. Zhang H, Zhou T, Yu Q, et al. pH-Sensitive betulinic acid polymer prodrug nanoparticles for efficient and targeted cancer cells treatment. *Int J Polym Mater*. 2020;69(10):659–668. doi:10.1080/00914037.2019.1596916
39. Zhu P, Luo W, Qian J, et al. GSH/ROS dual-responsive supramolecular nanoparticles based on pillar[6]arene and betulinic acid prodrug for chemodynamic combination therapy. *Molecules*. 2021;26(19):5900. doi:10.3390/molecules26195900
40. Saneja A, Kumar R, Minto MJ, et al. Gemcitabine and betulinic acid co-encapsulated PLGA-PEG polymer nanoparticles for improved efficacy of cancer chemotherapy. *Mater Sci Eng C-Mater*. 2019;98:764–771. doi:10.1016/j.msec.2019.01.026
41. Dai L, Cao X, Liu K, et al. Self-assembled targeted folate-conjugated eight-arm-polyethylene glycol-betulinic acid nanoparticles for co-delivery of anticancer drugs. *J Mater Chem B*. 2015;3(18):3754–3766. doi:10.1039/c5tb00042d
42. Lu S, Fan X, Wang H, et al. Synthesis of gelatin-based dual-targeted nanoparticles of betulinic acid for antitumor therapy. *ACS Appl Bio Mater*. 2020;3(6):3518–3525. doi:10.1021/acsabm.9b01204
43. Dai L, Si C. Cellulose-graft-poly(methyl methacrylate) nanoparticles with high biocompatibility for hydrophobic anti-cancer drug delivery. *Mater Lett*. 2017;207:213–216. doi:10.1016/j.matlet.2017.07.090
44. Dai L, Liu K, Si C, et al. Ginsenoside nanoparticle: a new green drug delivery system. *J Mater Chem B*. 2016;4(3):529–538. doi:10.1039/c5tb02305j
45. Dai L, Liu K, Si C, He J, Lei J, Guo L. A novel self-assembled targeted nanoparticle platform based on carboxymethylcellulose co-delivery of anticancer drugs. *J Mater Chem B*. 2015;3(32):6605–6617. doi:10.1039/c5tb00900f
46. Fu S, Wang M, Li B, et al. Bionic natural small molecule co-assemblies towards targeted and synergistic Chemo/PDT/CDT. *Biomater Res*. 2023;27(1):43. doi:10.1186/s40824-023-00380-z
47. Cheng J, Zhao H, Li B, et al. Photosensitive pro-drug nanoassemblies harboring a chemotherapeutic dormancy function potentiates cancer immunotherapy. *Acta Pharm Sin B*. 2023;13(2):879–896. doi:10.1016/j.apsb.2022.06.008
48. Özdemir Z, Yang M, Kim G, et al. Redox-responsive nanoparticles self-assembled from porphyrin-betulinic acid conjugates for chemo- and photodynamic therapy. *Dyes Pigm*. 2021;190:109307. doi:10.1016/j.dyepig.2021.109307
49. Chang Y, Jiao Y, Li D, Liu X, Han H. Glycosylated zein as a novel nanodelivery vehicle for lutein. *Food Chem*. 2021;376:131927. doi:10.1016/j.foodchem.2021.131927
50. Elzoghby AO, Samy WM, Elgindy NA. Albumin-based nanoparticles as potential controlled release drug delivery systems. *J Control Release*. 2012;157(2):168–182. doi:10.1016/j.jconrel.2011.07.031
51. Zheng B, Chen Y, Niu L, et al. Modulating the tumoral SPARC content to enhance albumin-based drug delivery for cancer therapy. *J Control Release*. 2024;366:596–610. doi:10.1016/j.jconrel.2023.12.057
52. Gupta R, Paul K. Investigating the serum albumin binding behavior of naphthalimide based fluorophore conjugates: spectroscopic and molecular docking approach. *ChemMedChem*. 2024;19(15):e202400114. doi:10.1002/cmdc.202400114
53. Tan T, Yang Q, Chen D, et al. Chondroitin sulfate-mediated albumin Corona nanoparticles for the treatment of breast cancer. *Asian J Pharm Sci*. 2021;16(4):508–518. doi:10.1016/j.ajps.2021.03.004
54. Adhikari C. Polymer nanoparticles-preparations, applications and future insights: a concise review. *Polym-Plast Technol*. 2021;60(18):1996–2024. doi:10.1080/25740881.2021.1939715
55. Cheng J, Zhao H, Wang J, Han Y, Yang X. Bioactive natural small molecule-tuned coassembly of photosensitive drugs for highly efficient synergistic and enhanced type I photochemotherapy. *ACS Appl Mater Inter*. 2020;12(39):43488–43500. doi:10.1021/acsami.0c13164
56. Liu Y, Gao D, Zhang X, et al. Antitumor drug effect of betulinic acid mediated by polyethylene glycol modified liposomes. *Mater Sci Eng C-Mater*. 2016;64:124–132. doi:10.1016/j.msec.2016.03.080
57. Wang G, Yu Y, Wang Y, Zhu Z, Yin P, Xu K. Effects and mechanisms of fatty acid metabolism-mediated glycolysis regulated by betulinic acid-loaded nanoliposomes in colorectal cancer. *Oncol Rep*. 2020;44(6):2595–2609. doi:10.3892/or.2020.7787
58. Farcas CG, Dehelean C, Pinzaru IA, et al. Thermosensitive betulinic acid-loaded magnetoliposomes: a promising antitumor potential for highly aggressive human breast adenocarcinoma cells under hyperthermic conditions. *Int J Nanomed*. 2020;15:8175–8200. doi:10.2147/IJN.S269630
59. Liu Y, Zhang X, Liu Z, et al. Gold nanoshell-based betulinic acid liposomes for synergistic chemo-photothermal therapy. *Nanomedicine*. 2017;13(6):1891–1900. doi:10.1016/j.nano.2017.03.012
60. Liu Y, Zhang X, Luo L, et al. Self-assembly of stimuli-responsive Au–Pd bimetallic nanoflowers based on betulinic acid liposomes for synergistic chemo-photothermal cancer therapy. *ACS Biomater Sci Eng*. 2018;4(8):2911–2921. doi:10.1021/acsbiomaterials.8b00766
61. Wu X, Wei Z, Feng H, et al. Targeting effect of betulinic acid liposome modified by hyaluronic acid on hepatoma cells in vitro. *J Pharm Sci*. 2022;111(11):3047–3053. doi:10.1016/j.xphs.2022.06.015
62. Guo B, Xu D, Liu X, Yi J. Enzymatic synthesis and in vitro evaluation of folate-functionalized liposomes. *Drug Des Devel Ther*. 2017;11:1839–1847. doi:10.2147/DDDT.S132841
63. Li C, Wang Z, Zhang Y, et al. Efficient sequential co-delivery nanosystem for inhibition of tumor and tumor-associated fibroblast-induced resistance and metastasis. *Int J Nanomed*. 2024;19:1749–1766. doi:10.2147/IJN.S427783
64. Chen X, Lu S, Gong F, Sui X, Liu T, Wang T. Research on the synthesis of nanoparticles of betulinic acid and their targeting antitumor activity. *J Biomed Mater Res B*. 2022;110(8):1789–1795. doi:10.1002/jbm.b.35036



65. Wang G, Yang Y, Yi D, et al. Eudragit S100 prepared pH-responsive liposomes-loaded betulinic acid against colorectal cancer in vitro and in vivo. *J Liposome Res.* **2022**;32(3):250–264. doi:10.1080/08982104.2021.1999974
66. Shu Q, Wu J, Chen Q. Synthesis, characterization of liposomes modified with biosurfactant MEL-A loading betulinic acid and its anticancer effect in HepG2 cell. *Molecules.* **2019**;24(21):3939. doi:10.3390/molecules24213939
67. Rodríguez-Luccioni HL, Latorre-Esteves M, Méndez-Vega J, et al. Enhanced reduction in cell viability by hyperthermia induced by magnetic nanoparticles. *Int J Nanomed.* **2011**;6:373–380. doi:10.2147/IJN.S14613
68. Farzin A, Etesami SA, Quint J, Memic A, Tamayol A. Magnetic nanoparticles in cancer therapy and diagnosis. *Adv Health Mater.* **2020**;9(9):e1901058. doi:10.1002/adhm.201901058
69. Li J, Zhang W, Ji W, et al. Near infrared photothermal conversion materials: mechanism, preparation, and photothermal cancer therapy applications. *J Mater Chem B.* **2021**;9(38):7909–7926. doi:10.1039/d1tb01310f
70. Zhang W, Huang X. Stem cell membrane-camouflaged targeted delivery system in tumor. *Mater Today Bio.* **2022**;16:100377. doi:10.1016/j.mtbio.2022.100377
71. Lin M, Dai Y, Xia F, Zhang X. Advances in non-covalent crosslinked polymer micelles for biomedical applications. *Mater Sci Eng C-Mater.* **2021**;119:111626. doi:10.1016/j.msec.2020.111626
72. Biswas S, Kumari P, Lakhani PM, Ghosh B. Recent advances in polymeric micelles for anti-cancer drug delivery. *Eur J Pharm Sci.* **2016**;83:184–202. doi:10.1016/j.ejps.2015.12.031
73. Jin X, Zhou J, Zhang Z, Lv H. Doxorubicin combined with betulinic acid or lonidamine in RGD ligand-targeted pH-sensitive micellar system for ovarian cancer treatment. *Int J Pharm.* **2019**;571:118751. doi:10.1016/j.ijpharm.2019.118751
74. Hou J, Sun E, Sun C, et al. Improved oral bioavailability and anticancer efficacy on breast cancer of paclitaxel via Novel Soluplus®—Solutol® HS15 binary mixed micelles system. *Int J Pharm.* **2016**;512(1):186–193. doi:10.1016/j.ijpharm.2016.08.045
75. Qi X, Gao C, Yin C, Fan J, Wu X, Guo C. Improved anticancer activity of betulinic acid on breast cancer through a grafted copolymer-based micelles system. *Drug Deliv.* **2021**;28(1):1962–1971. doi:10.1080/10717544.2021.1979125
76. Zhang Y, Zhou H, Zhang Z, et al. Redox/NIR dual-responsive PEG-betulinic acid/pluronic-cypate prodrug micelles for chemophotothermal therapy. *Colloids Surf A.* **2021**;609:125662. doi:10.1016/j.colsurfa.2020.125662
77. Qu H, Yang J, Li S, et al. Programmed-response cross-linked nanocarrier for multidrug-resistant ovarian cancer treatment. *J Control Release.* **2023**;357:274–286. doi:10.1016/j.jconrel.2023.03.031
78. Gautam S, Marwaha D, Singh N, et al. Self-assembled redox-sensitive polymeric nanostructures facilitate the intracellular delivery of paclitaxel for improved breast cancer therapy. *Mol Pharm.* **2023**;20(4):1914–1932. doi:10.1021/acs.molpharmaceut.2c00673
79. Lomkova EA, Chytil P, Janoušková O, et al. Biodegradable micellar HPMA-based polymer-drug conjugates with betulinic acid for passive tumor targeting. *Biomacromolecules.* **2016**;17(11):3493–3507. doi:10.1021/acs.biomac.6b00947
80. Lei W, Sun C, Jiang T, et al. Polydopamine-coated mesoporous silica nanoparticles for multi-responsive drug delivery and combined chemophotothermal therapy. *Mater Sci Eng C-Mater.* **2019**;105:110103. doi:10.1016/j.msec.2019.110103
81. Tan JM, Karthivashan G, Arulselvan P, Fakurazi S, Hussein MZ. Characterization and in vitro studies of the anticancer effect of oxidized carbon nanotubes functionalized with betulinic acid. *Drug Des Devel Ther.* **2014**;8:2333–2343. doi:10.2147/DDDT.S70650
82. Dai L, Liu R, Hu L, Wang J, Si C. Self-assembled PEG-carboxymethylcellulose nanoparticles/ $\alpha$ -cyclodextrin hydrogels for injectable and thermosensitive drug delivery. *RSC Adv.* **2017**;7(5):2905–2912. doi:10.1039/c6ra25793c
83. Dai L, Liu K, Wang L, et al. Injectable and thermosensitive supramolecular hydrogels by inclusion complexation between binary-drug loaded micelles and  $\alpha$ -cyclodextrin. *Mater Sci Eng C-Mater.* **2017**;76:966–974. doi:10.1016/j.msec.2017.03.151
84. Dash SK, Dash SS, Chattopadhyay S, et al. Folate decorated delivery of self assembled betulinic acid nano fibers: a biocompatible anti-leukemic therapy. *RSC Adv.* **2015**;5(31):24144–24157. doi:10.1039/C5RA01076D
85. Dash SK, Chattopadhyay S, Tripathy S, et al. Self-assembled betulinic acid augments immunomodulatory activity associates with IgG response. *Biomed Pharmacother.* **2015**;75:205–217. doi:10.1016/j.biopha.2015.07.033
86. Rebouças LM, Sousa ACC, Sampaio CG, et al. Microcapsules based on alginate and guar gum for co-delivery of hydrophobic antitumor bioactives. *Carbohydr Polym.* **2023**;301(Pt A):120310. doi:10.1016/j.carbpol.2022.120310
87. Pinzaru I, Sarau C, Coricovac D, et al. Silver nanocolloids loaded with betulinic acid with enhanced antitumor potential: physicochemical characterization and in vitro evaluation. *Nanomaterials.* **2021**;11(1):152. doi:10.3390/nano11010152
88. Li S, Zhang J, Fang Y, et al. Enhancing betulinic acid dissolution rate and improving antitumor activity via nanosuspension constructed by anti-solvent technique. *Drug Des Devel Ther.* **2020**;14:243–256. doi:10.2147/DDDT.S233851
89. Wang R, Yang M, Li G, et al. Paclitaxel-betulinic acid hybrid nanosuspensions for enhanced anti-breast cancer activity. *Colloids Surf B.* **2019**;174:270–279. doi:10.1016/j.colsurfb.2018.11.029
90. Wang R, Wang X, Jia X, Wang H, Li W, Li J. Impacts of particle size on the cytotoxicity, cellular internalization, pharmacokinetics and biodistribution of betulinic acid nanosuspensions in combined chemotherapy. *Int J Pharm.* **2020**;588:119799. doi:10.1016/j.ijpharm.2020.119799
91. Mehra NK, Jain NK. Multifunctional hybrid-carbon nanotubes: new horizon in drug delivery and targeting. *J Drug Target.* **2016**;24(4):294–308. doi:10.3109/1061186X.2015.1055571
92. Tan JM, Karthivashan G, Abd Gani S, Fakurazi S, Hussein MZ. Biocompatible polymers coated on carboxylated nanotubes functionalized with betulinic acid for effective drug delivery. *J Mater Sci.* **2016**;27(2):26. doi:10.1007/s10856-015-5635-8
93. Merino S, Martín C, Kostarelos K, Prato M, Vázquez E. Nanocomposite hydrogels: 3D polymer–nanoparticle synergies for on-demand drug delivery. *ACS Nano.* **2015**;9(5):4686–4697. doi:10.1021/acsnano.5b01433
94. Ahmed A, Sarwar S, Hu Y, et al. Surface-modified polymeric nanoparticles for drug delivery to cancer cells. *Expert Opin Drug Deliv.* **2021**;18(1):1–24. doi:10.1080/17425247.2020.1822321
95. Dash SK, Chattopadhyay S, Dash SS, et al. Self assembled nano fibers of betulinic acid: a selective inducer for ROS/TNF- $\alpha$  pathway mediated leukemic cell death. *Bioorg Chem.* **2015**;63:85–100. doi:10.1016/j.bioorg.2015.09.006
96. Dash SK, Chattopadhyay S, Ghosh T, et al. Self-assembled betulinic acid protects doxorubicin induced apoptosis followed by reduction of ROS–TNF- $\alpha$ –caspase-3 activity. *Biomed Pharmacother.* **2015**;72:144–157. doi:10.1016/j.biopha.2015.04.017
97. Meng Q, Zhong S, Gao Y, Cui X. Advances in polysaccharide-based nano/microcapsules for biomedical applications: a review. *Int J Biol Macromol.* **2022**;220:878–891. doi:10.1016/j.ijbiomac.2022.08.129



98. Ahmadian E, Dizaj SM, Rahimpour E, et al. Effect of silver nanoparticles in the induction of apoptosis on human hepatocellular carcinoma (HepG2) cell line. *Mater Sci Eng C-Mater*. 2018;93:465–471. doi:10.1016/j.msec.2018.08.027
99. Ma Y, Cong Z, Gao P, Wang Y. Nanosuspensions technology as a master key for nature products drug delivery and In vivo fate. *Eur J Pharm Sci*. 2023;185:106425. doi:10.1016/j.ejps.2023.106425

### International Journal of Nanomedicine

### Publish your work in this journal

The International Journal of Nanomedicine is an international, peer-reviewed journal focusing on the application of nanotechnology in diagnostics, therapeutics, and drug delivery systems throughout the biomedical field. This journal is indexed on PubMed Central, MedLine, CAS, SciSearch®, Current Contents®/Clinical Medicine, Journal Citation Reports/Science Edition, EMBase, Scopus and the Elsevier Bibliographic databases. The manuscript management system is completely online and includes a very quick and fair peer-review system, which is all easy to use. Visit <http://www.dovepress.com/testimonials.php> to read real quotes from published authors.

Submit your manuscript here: <https://www.dovepress.com/international-journal-of-nanomedicine-journal>

**Dovepress**  
Taylor & Francis Group